A STUDY OF THE UTILIZATION OF PANEL METHOD FOR LOW ASPECT RATIO WING ANALYSIS

A Thesis

presented to

the Faculty of California Polytechnic State University,

San Luis Obispo

In Partial Fulfillment

of the Requirements for the Degree

Master of Science in Aerospace Engineering

by

William B. D. Newey

June 2020

COMMITTEE MEMBERSHIP

TITLE:	A Study of the Utilization of Panel Method for Low Aspect Ratio Wing Analysis
AUTHOR:	William B. D. Newey
DATE SUBMITTED:	May 2020
COMMITTEE CHAIR:	Paulo Iscold, Ph.D. Professor of Aerospace Engineering
COMMITTEE MEMBER:	Aaron Drake, Ph.D. Professor of Aerospace Engineering
COMMITTEE MEMBER:	David Marshall, Ph.D Professor of Aerospace Engineering
COMMITTEE MEMBER:	Kurt Colvin, Ph.D. Professor of Systems Engineering

ABSTRACT

A Study of the Utilization of Panel Method for Low Aspect Ratio Wing Analysis
William B. D. Newey

This study demonstrates the applicability of using a modified application strategy of panel method to analyze low aspect ratio wings at preliminary design phases. Conventional panel methods fail to capture the leading edge vortex (LEV) that is shed by wings with low aspect ratios, typically below 2 depending on planform. This aerodynamic phenomenon contributes to a significant amount of the lift of these wings and the result is a drastic underestimation of the lift characteristics when analyzed by conventional panel method. To capture the effect of the leading edge vortex, a panel method code was used with an extended definition of the Kutta condition along portions of the leading edge inducing a vortex to shed from the leading edge and flow aft just inside the leading edge. To validate that this method, it was applied to 2 elliptical planforms with constant thickness where experimental force balance data was available. Additionally, the same 2 wings were analyzed using a finite volume solver to compare pressure distributions and to demonstrate the difference in magnitude of solution times. For comparison purposes, the resulting forces and moments from both computational methods and experimental testing were plotted over a range of angles of attack. Overall, the results demonstrate that a modified panel method could be used during the preliminary design phases for low aspect ratio wings. The panel method can reasonably model the lift and induced drag characteristics of low aspect ratio wings. This method loses applicability beyond the stall point where the leading edge vortex breaks down and oversimplifies pitching moment relation to angle of attack. Additionally, when compared to finite volume solutions of the same scenario, the panel method provided a result 20 to 30 times faster than the finite volume solutions. With this in mind, the modified panel method application strategy lends itself to preliminary design phases of low aspect ratio wings where the level of detail does not warrant finite volume analysis and solution speed has higher priority.

Keywords: Panel Method, Low Aspect Ratio, Computational Fluid Dynamics, CFD, Zimmerman Planform, Leading Edge Vortex

ACKNOWLEDGMENTS

I would like to thank everyone who aided in my educational success. I would not have been able to accomplish what I have without the years of public education and extracurricular advising I received from educators, coaches, and supporters.

I would especially like to thank Paulo Iscold for being an excellent advisor whose passion for the subject inspires me. Without your support, I would not have the same appreciation for my own quality of work or my own passion for aeronautics and aircraft design.

I would also like to thank my family for all of the financial, emotional, and other support they have given me throughout my life. My parents provided some of the best career and educational advice through example in their own lives. I hope to accomplish so much more after this educational stepping stone and follow in your footsteps by having a successful career.

I would also like to thank my close friends and my partner, Georgina, for being supportive throughout the long nights and busy weekends. Without your continued emotional and mental support, I would not have been able to accomplish what I did.

Lastly, I would like to thank Cal Poly for all of the programs and resources they provided me which allowed me to complete my thesis. Without access to these programs and resources, I would not have been able to complete this work.

TABLES OF CONTENTS

LIST OF TABLES

Table Page

LIST OF FIGURES

Figure Page

1. INTRODUCTION

Aspect ratio is a geometric feature of a wing that compares the span to the average chord length. It is a nondimensional design parameter that has significant effects on almost all performance metrics for an aircraft. Low Aspect Ratio (LAR) wings, which are typically less than 2, have unique performance characteristics that are useful for specific missions/applications. The aerodynamic design analysis of LAR wings is difficult and time consuming. Most of the aerodynamic design is based on empirical relations from wind tunnel data and/or time intensive finite volume solutions [1][2]. A possible solution for the design of these wings, at low Mach numbers, could be using potential flow solvers like vortex lattice or panel methods. A different application strategy of a conventional panel method is a possible solution for preliminary phase aerodynamic design of LAR wings because they can model aerodynamic trends with a level of accuracy that matches the design maturity in a significantly quicker time than finite volume solutions.

This chapter presents the necessary background information to understand the issues with designing LAR wings as well as why they might be considered for an aircraft design. First, an overview of the characteristics of LAR wings, utility, design applications, and aerodynamics is presented. The characteristics of LAR wings help explain the overall costs and benefits of using this type of wing. Next, this chapter summarizes the research associated with this panel method application strategy. Finally, the purpose and objectives of the research are presented which is to demonstrate the applicability of a unconventional panel method application strategy for preliminary design phases for LAR aircraft design.

1.1 Low Aspect Ratio Wings

Low aspect ratio wings provide unique flight characteristics that could be beneficial in particular applications. Typical applications take advantage of the lower wave drag they provide at high Mach numbers or the lower empty weight that they sometimes provide[1][2]. The field of aerodynamics has a significant lack of preliminary design tools for analyzing these wings at design phases where the level of detail of the design does not merit the computational cost or fidelity of answer. This section gives insight into LAR wings characteristics by outlining their utility, design applications, and aerodynamics. Likewise, this section highlights the benefits of using a LAR wing

for design, overviews the various applications of LAR wings, and outlines some of the associated aerodynamic phenomena.

1.1.1 Utility

The success of any wing design comes from the leveraging of wing characteristics to obtain the desired performance. There are several types of aircraft performance metrics that are desirable; overall design performance is typically measured in structural, propulsive, and aerodynamic efficiency as well as stability and controllability [1][2]. All design decisions effect the performance in each of the metrics, often in interconnected ways. Something as major as a wing's aspect ratio (AR), has drastic effects on the overall performance of a wing in all measures. To understand the full utility of having a low aspect ratio (LAR) wing, it is necessary to understand the performance effects of applying it to the correct mission.

An aircraft's aerodynamic efficiency, measured in lift to drag ratio, decreases with aspect ratio [1][2]. Discussed later in the Aerodynamics (1.1.3) section, a LAR wing can provide the lift necessary for all portions of flight but only at high angles of attack and increased drag. This combination leads to low lift to drag ratios. This is usually a negative characteristic of an aircraft as it means more power must be added to the system to maintain flight [1][2]. However, this can be desirable in certain applications which require steep approach angles. Additionally, LAR wings have high departure resistance and are forgiving to relatively inexperienced pilots. The stall can be gentle and at such a drastic angle of attack that a pilot would have difficulty achieving it or not noticing that it occurred. LAR wing's implicitly have decreased aerodynamic efficiency, however, they offer unique flight qualities that could prove beneficial in certain applications [1][2][3].

An aircraft's structural efficiency typically increases with aspect ratio. This is measured by a decreasing empty weight fraction with decreasing aspect ratio [1][2]. As the aspect ratio increases, the structure within a wing converges to a beam-like solution because the chord and thickness become too small to support other options. As the aspect ratio decreases, the structure within the wing has more ambiguity for frame and truss-like solutions. Even with more members, the overall structure can be significantly lighter to support the same loads. Additionally, as the aspect ratio becomes even lower, major aircraft structures combine forming blended-wing body

shapes. Besides lower empty weight, this additionally can offer more room for payload or pilot and lower the overall part count of the aircraft, simplifying the construction/manufacturing. In general, as the aspect ratio of an aircraft decreases, the structural weight decreases while still sustaining the same aerodynamic loads.

The propulsive efficiency is not dependent on the aspect ratio of the aircraft and is more strongly determined by the choice of engine type/model, intake design, and exhaust design. A concern worth noting, is the possibility of decreased performance (both efficiency and thrust) when there is a high incidence of the intake or propeller(s) to the freestream flow [1][2]. This situation would occur when the LAR aircraft is at high lift scenarios like take-off, approach, and landing. The remedy for this design problem requires analysis specific to the aircraft and will not be covered in this paper.

Stability is largely not driven by aspect ratio, but because of the geometric effects on an aircraft's configuration, the aspect ratio has major contributions to the overall stability of an aircraft. The largest contribution the aspect ratio makes to longitudinal stability is the large increase in length of the root and mean aerodynamic chord (MAC) [4]. Typically, an aircraft is stable if the total center of gravity is within an envelope along the MAC of the wing. For example, this might be a range between 25-50% of the total length of the MAC. That range would scale with the length of the MAC; if the MAC is significantly longer, like in the case of a LAR wing, this range is larger. This allows for greater flexibility and/or larger margins in loading a LAR aircraft.

The greatest utility for a LAR aircraft will be seen when designed for a mission that has specific performance needs. That mission will either have a high Mach number portion of the mission or will take advantage of the unique aerodynamic characteristics LAR wings offer. In high speed applications LAR wings offer lower wave drag [1][2]. At lower (incompressible) speed the application of a LAR wing will have greater value on stability and controllability for relatively inexperienced pilots and less value from aerodynamic and propulsive efficiency. Additionally, this mission would have requirements and gain value from steep approach angles. Benefits from LAR aircraft that are not mission specific would include a lower part count; this could lead to decreased manufacturing cost and a lighter/less expensive aircraft overall. A LAR aircraft design will only seem

useful if it is applied to a mission that values the characteristics of LAR wings, otherwise, the application would provide performance characteristics that aren't valued and may fall short in other categories.

1.1.2 Design Applications

There are many examples of successful applications of LAR wings. A significant number of these applications were to take advantage of the lower wave drag that accompanies a lower aspect ratio at higher Mach numbers [1][2][5]. Notable examples include Spaceship 1, F-35, Space Shuttle, and Concorde, pictured in Figure 1.1. The lower aspect ratio of these aircraft significantly reduces wave drag and structural loads on the aircraft. It is important to note that even though these aircraft typically operate at high speeds, the conditions in which these vehicles land is significantly slower and falls within the regime where the flow can be considered incompressible and the leading edge vortex phenomenon can be observed [6].

Even though this landing condition is a small portion of the vehicle's total flight time, this condition can constrain high speed aircraft design. For example, the nose droop that was emblematic of the Concorde during landing sequence was a concession made to allow the pilots to see on approach at such drastic angles of attack (AoA) (Figure 1.2). This drastic angle was necessary to achieve the required lift during approach due to the low aspect ratio that also allowed for supersonic cruise. If the aspect ratio were to have been higher, the lift required during approach could be achieved with a lower AoA and the nose would not have to droop. However, this would have come at the cost of increased drag at the supersonic cruise condition. Better analysis tools at the early wing design phases could have allowed for wing that both reduced wave drag at the cruise condition and met a lower required approach AoA.

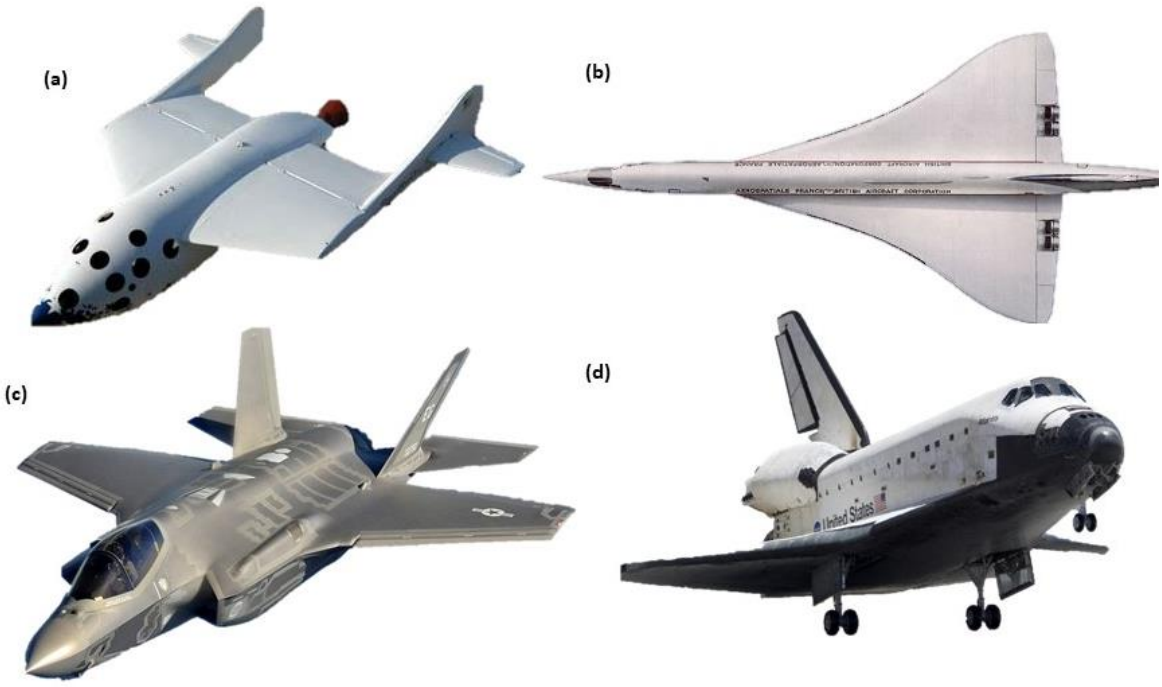

Figure 1.1 Various High Mach Number Applications of LAR wings
(a) Spaceship One [7] (b) Concorde [8] (c) Lockheed Martin F-35 [9](d) Space Shuttle Orbiter [10]

Figure 1.2 Concorde during Approach
Notice the nose which is drooped to allow for increased visibility at the approach AoA. [11]

Not all aircraft with LAR wings are for high Mach number applications. There are notable exceptions that attempted to take advantage of the weight savings and unique low speed aerodynamics of LAR wings. The Vought V-173, Dyke Delta, and Wainfran Facetmobile, pictured in Figure 1.3, were examples of successful applications of LAR wings whose mission took advantage of the characteristics of LAR wings. The Dyke Delta and Wainfran Facetmobile were designed with the intent of reducing the overall weight, part count, and cost of the aircraft to make air travel more accessible to the public [12][13]. The Facetmobile weighed only 710 pounds, which is only 29% the weight of a Cessna 172, the standard general aviation competitor [14]. It should be

noted, however, that this aircraft was an experimental demonstrator and was not constructed with longevity in mind. The manufacturing cost and weight savings that Wainfran boasts might be an overestimate when compared to a production version cost and weight but it represents the possible advantages of LAR wings.

These aircraft's aerodynamic efficiency suffers because of the LAR, but because the user is a general aviation pilot, this characteristic is not as significant to the mission. In fact, these aircraft were advertised for their steep approach angles, slow landing speeds, and departure resistance that result from the unique aerodynamics characteristics of their LAR wings. The aerodynamic efficiency toll could be reduced if the wings took full advantage of the LEV that provides their lift.

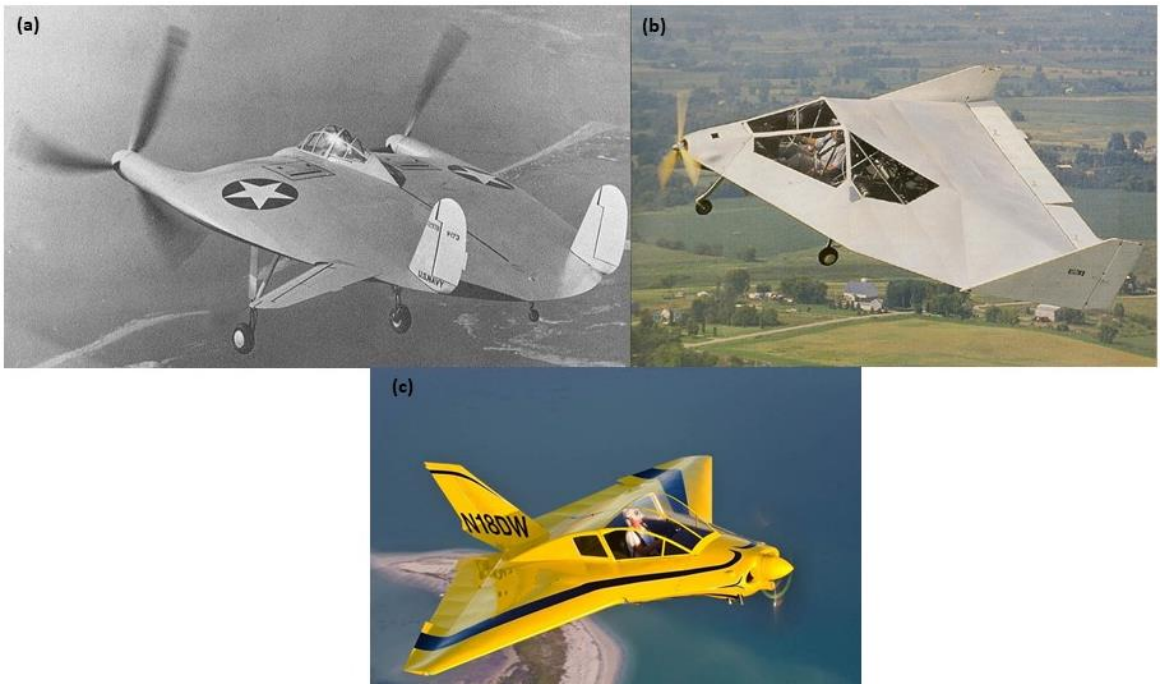

Figure 1.3 Various Low Speed Applications of LAR wings
(a) Vought V-173 [15] (b) Wainfran Facetmobile [12] (c) Dyke Delta [16]

Improved early development tools would allow for more finely tuned LAR wings that take advantage of the weight savings and aerodynamic characteristics without the degradation in aerodynamic efficiency during cruise. Panel method solutions are a traditional technique used at this intermediate phase of the design process but would not capture the LEV phenomenon that produces a significant amount of the lift seen in LAR wings. If a modification to the panel method could allow for better modelling of the flow around LAR wings, the design of a LAR aircraft could

be done much more rapidly without time wasted using costly finite volume solutions on geometry that does not have the level of detail necessary for useful solutions.

1.1.3 Aerodynamics

Typically, as the aspect ratio of a finite wing decreases, the slope of the C_L versus angle of attack (AoA) curve decreases and to obtain the same lift coefficient, the wing must be at a higher AoA (Figure 1.4) [3][17][18][19][20][21]. However, an interesting phenomenon occurs with wings that have an AR below approximately 1.5. The maximum lift coefficient for these wings can be significantly higher than predicted when following trends of higher AR wings. This increased lift is caused by the formation of a vortex shed consistently from the leading edge of the wing.

For analysis, LAR wings can be split into those that have swept leading edges and those that do not. The wings that do not exhibit global sweep can have local sweep that can vary. An example would be an elliptical wing, where locally, at one point on the leading edge, the planform edge can have an incidence angle to the freestream direction and could be thought of as being swept. Observing a different point would reveal a different local sweep. When applying this idea to the same shape with a higher aspect ratio would reveal a larger portion of the wing that is nearly perpendicular to the freestream direction and has no sweep.

LAR wings with no sweep (i.e. rectangular planforms) shed LEV periodically, alternating with the trailing edge [22][23]. This LEV is not a steady phenomenon and resembles the oscillatory vortex shedding seen by bluff bodies governed by Strouhal number [22][23][24]. Because this type of flow field cannot be modelled as steady, it is not conducive to the modelling techniques used in this research and therefore will not be discussed/modelled in this paper.

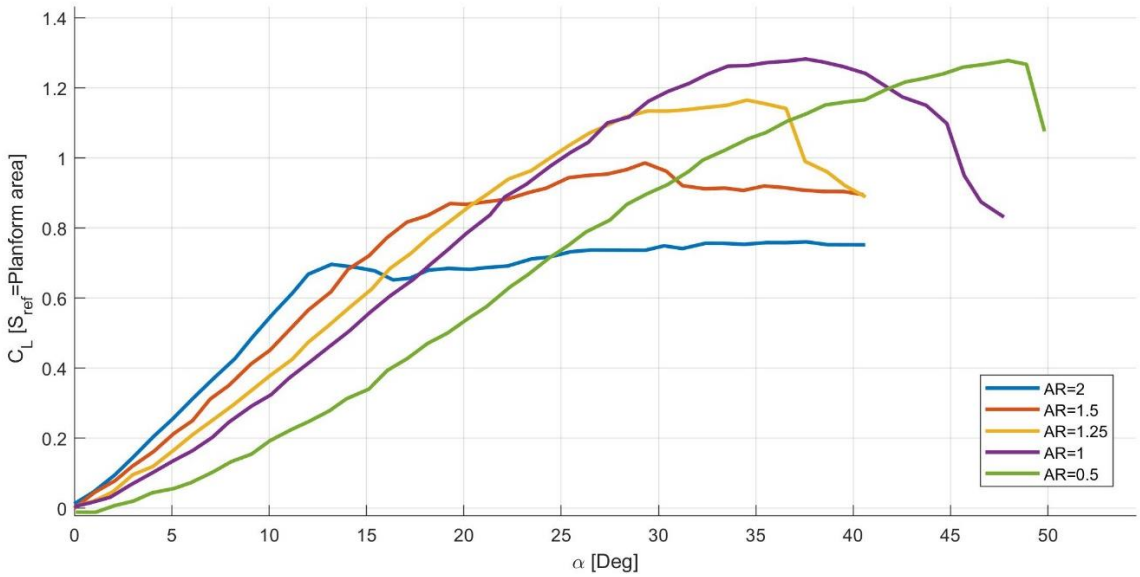

Figure 1.4 Experimental Lift Curves of Circular Tip Wings Adapted from [17].

LAR wing with leading edge sweep will shed a LEV consistently and exhibit steady flow characteristics. For these wings, the LEV is shed and flows back just inside the leading edge (Figure 1.5) [6]. This acceleration of the flow accompanies a decrease in pressure under the LEV and an increase in the total lift coefficient for the wing. Because this flow phenomenon occurs at relatively high angles of attack, this also results in significantly increased induced drag. At even higher angles of attack, the LEV breaks down causing the wing to stall; the stall for LAR wings typically is extremely gentle and can be difficult to achieve in application.

It is important to keep in mind that all of the aerodynamics discussed in this paper deal with relatively low speed/Mach number (<0.2) even though a significant number of LAR wings are utilized for higher Mach numbers with swept leading edges [1][2][6][25]. The analysis presented, however, still has applicability to these same aircraft. The landing conditions for these aircraft typically fall within the low speed flow assumptions and the same LEV flow phenomenon can be observed [6][25].

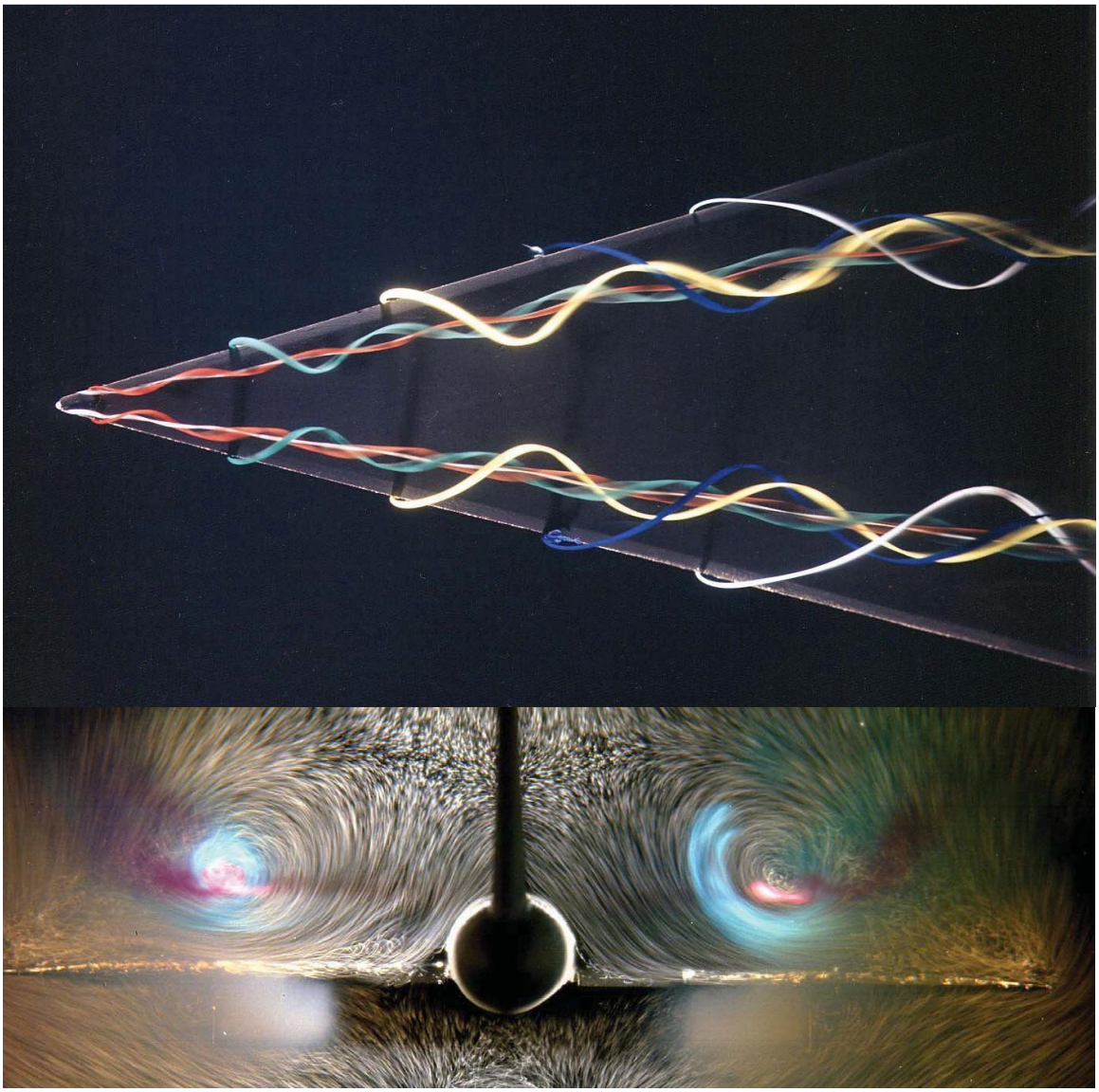

Figure 1.5 Flow Visualizations over a Delta wing and a Concorde model at Increased AoA

Potential flow solvers like lifting line, vortex lattice and vortex panel method are early stage design tools that capture the lift loss as the aspect ratio decreases but have limited applicability at lower aspect ratios [26]. The applicability of these solution techniques falls short at low aspect ratios because they do not account for the leading-edge vortex and the accompanying lift (Figure 1.6) [20]. The results can be adjusted using experimentally determined coefficients to allow for them to be more useful for early design calculations. These corrections are trying to capture the effect of the lift caused by the steady shedding of a LEV. This lift, described by the Polhamus suction analogy, is generated at high AoA where traditional wings have stalled (>20°) for wing with aspect ratio less than ~1.5. The LEV sheds consistently and predictably based on experimental

observations; various studies have done parametric studies showing the effects of leading-edge curvature, sweep angle, and Reynolds Number [3][12][19][27].

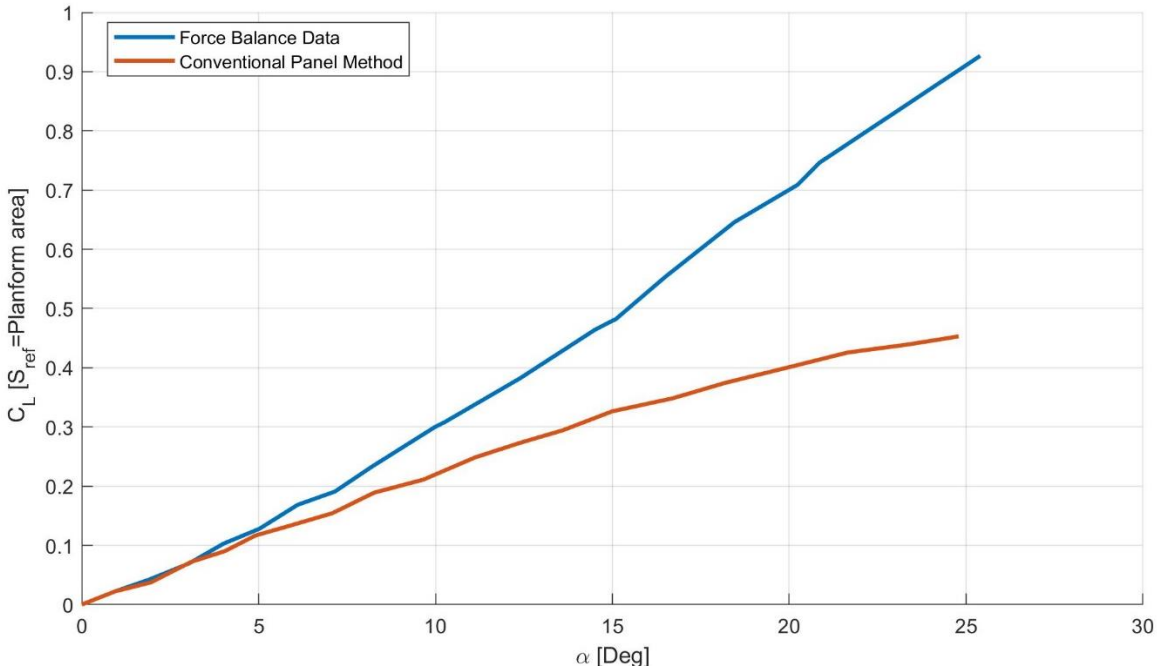

Figure 1.6 Lift coefficient data for an AR 1 flat plate delta wing
Notice how conventional panel methods don't capture the lift caused by LEV, adapted from [20].

1.2 Project Purpose & Objectives

The purpose of my thesis is to demonstrate the feasibility of a different application strategy for panel method can be used to model low aspect ratio wings at subsonic conditions. When successful, this application strategy of panel method has applications in the preliminary design of a LAR aircraft with the advantage of the shorter development times.

To successfully demonstrate the feasibility of this application strategy of panel method to generic LAR wings, several milestones must be met and will guide the methodology used throughout the project:

1. Generic LAR wing geometries and flight conditions must be selected based on available experimental reference data. By analyzing wings that have been observed in wind tunnel testing, the numerically obtained results can be compared and validated.
2. Selected wing shapes must be analyzed using a conventional panel method approach as well as using the different application strategy of panel method. By comparing the results

of the two panel method application strategies, the effect of the modification can be visualized through lower lift coefficients and variance in calculated pressure distributions.

3. The same generic wings should be analyzed using a higher fidelity finite volume solver. This will demonstrate the larger time/computational requirement of this method as well as provide comparison to the conventional and modified application strategies of panel method solutions. This analysis will give additional comparisons that cannot be made with the experimental reference data alone.
4. The resulting forces and pressure distributions obtained from both panel methods will be compared to experimental data for resulting lift forces and to the finite volume solution for pressure distributions and flow phenomenon. This objective demonstrates the level of accuracy of the modified application strategy of panel method and ultimately the usability in the design process.
5. Lastly, a comparison between the finite volume and panel method solution times will be made to assess the advantage of panel methods in preliminary LAR wing design.

When successful, this project will demonstrate the feasibility of a modified application of panel method can be used for the design of low aspect ratio wings before turning to higher fidelity and more computationally expensive methods like finite volume solutions.

2. METHODOLOGY

This chapter outlines the analysis that was done for this project. The different application strategy of panel method is presented with the accompanying limitations and expected results. Next, the chosen geometry is discussed as well as how the various analysis techniques were applied in order to demonstrate the applicability of a modified application strategy of panel method to the design of LAR wings. Additionally, mesh refinement studies are presented to demonstrate that the methods were applied at a fine enough discretization to yield accurate results.

2.1 Panel Method Adaptation

The use of empirical relations, wind tunnel experiments, and finite-volume simulations are the dominate tool for design for these LAR wings [1][2]. All of these analysis tools end up being either too low or too high fidelity for early stage aerodynamic design for these wings. The level of detail of the designs does not match the analysis tool leading to wasted time during the design process.

Conventional panel methods are a computational analysis technique that does not capture the LEV flow phenomenon of LAR wings. It is typically a medium fidelity solution during the design process and balances the level of detail and the need for higher fidelity analysis than vortex lifting line and empirical. Other investigations have revealed this method can be modified in a way that can capture the LEV phenomenon but has not been applied widely enough to have confidence in this method or be predictive for design applications [23][26].

2.1.1 Vortex Panel Method

Panel methods are a numerical approach to solve Laplace's equation for a flow filed (eqn. 1.1) [13].

$$\nabla^2 \phi = 0 \tag{1.1}$$

There are numerous solutions to this differential equation and these solutions can be combined linearly and still satisfy the differential equation [28]. A common technique for modelling wings is to use vortex lifting line method. This is a superposition of 3 linear vortices segments, in a U-shape configuration, and a freestream flow. Each characteristic solution piece (the 3 vortex lines and a freestream flow) has an influence on every point in the flow field. To solve for flow conditions at any point in the flow field, each characteristic solution's influence is evaluated based on the

distance to the point of interest. A second approach will be the Vortex Lattice method (VLM). Similar to lifting line method, the VLM has higher fidelity by having more elements, normally distributed along the span and the chord. Just as any potential flow solver, to solve an any point, each line vortex of each U-shape must be considered. This method requires more calculations than vortex lifting line method but allows for higher fidelity modelling [5].

The next level of potential flow modelling technique is a panel method. This method approximates generic geometries into a set of panels. Each of these panels then has influence on every point in the flow. Because this method is higher fidelity, it has higher computational costs compared to lifting line and vortex lattice methods. This is because at each point where the user is interested in solving for, the influence of each panel must be solved for. Additionally, this method has a boundary condition at the geometry surface in which flow normal to the panel surface is zero. With the introduction of vorticity (through a vortex or dipole) the Laplacian requires 1 more boundary condition. There are many acceptable solutions to this, but most commonly the Kutta condition is implemented [5].

The Kutta condition is a mathematical boundary condition that forces smooth detachment of flow or a stagnation condition at the trailing edge of wings modelled using panel method [5]. This implies that the actual flow leaves the trailing edge smoothly and that the mathematical model has the same velocity on the top and bottom surface [5][23]. This condition is applied at the trailing edge of the geometry and typically captures the wing tip vortex effects that are observed on traditional wings of moderate aspect ratio.

As with any modelling technique, there are limitations and boundaries of where the method is applicable/accurate. Like all potential flow models, panel method cannot be used to estimate total drag. The inherent inviscid and irrotational assumptions disregard large contributions to the total drag. Because panel method is a potential method, it is unable to estimate drag or flow separation/stall [5][23]. Resultant force predictions from a panel method simulation would show linear relations between lift coefficient and AoA. Even though panel methods cannot estimate total drag, it would be expected that they would be able to estimate general trends in LAR drag characteristics. This is due to the fact that a significant amount of the drag produced by these wings

at high AoA is induced drag which is able to be captured by potential methods [20][22][23] [26]. It is important to understand these limitations when applying new panel method application strategies and using this method in design applications.

Conventional panel method are not used to model LAR wings as they do not capture the LEV phenomenon and therefore lose applicability/accuracy at aspect ratios below approximately 2. This is because the LEV phenomenon becomes a dominant source of lift [20][21]. Corrective coefficients can be applied conventional potential flow modelling to get better estimates for LAR wings, but this correction introduces a level of uncertainty that might be greater than the necessary fidelity for design. If a panel method could be applied in a way to capture the LEV phenomenon, it might have better applicability to later stage conceptual design where a higher level of fidelity is required before detailed design should begin.

2.1.2 Leading Edge Kutta Definition

The Kutta condition offers a possible strategy to apply to conventional panel method that could better capture the LEV caused by LAR wings at high angles of attack and has been demonstrated to work in other panel method investigations [5][23]. By defining the Kutta condition along portions of a swept (or locally swept) leading edge, a LEV could be induced. This has been shown to be effective in capturing the effect of the LEV in highly swept leading edges [23]. The application of this method to locally swept leading edges has not been demonstrated and has only been applied to globally swept wings [23].

Modifying the location of where the Kutta condition is applied comes with additional assumptions about the flow. Any flow phenomenon captured by this panel method (ex. LEV) would have to be caused by a potential flow phenomenon in the actual flow. By assuming that the leading edge vortex of a LAR wing can be modelled using a panel method, this would mean that the LEV is not caused by viscous effects. Additionally, because it has been observed that the LEV moves relative to the wing with variance in AoA and sideslip, the location of where the modified Kutta condition is applied would vary based on the these as well and not just upon the wing geometry [13][21][29]. If this modified application strategy of panel method can capture the LEV of LAR wings, the design of LAR aircraft could accelerate and allow for much faster prototyping.

2.2 Experimental Comparison

For experimental comparison, it is important that the comparison data is well documented throughout the process and has little uncertainty from experimental error. For this research, the wind tunnel experiments documented by Thomas J. Mueller were used [17]. In this paper, Mueller tests the aerodynamic performance characteristics of *Zimmerman* and elliptical planforms of constant thickness with varying edge shapes and Reynolds numbers. *Zimmerman* and elliptical planforms are good representations for generic planforms with local sweep of varying angles. This paper has in depth documentation to fully define the test geometry and conditions. Additionally, the relative recentness of the work and well documented error analysis merit more confidence when validating against the results of this paper.

2.2.1 Geometry

Two wing geometries and Reynolds numbers were chosen from this data; both inverse *Zimmerman* planform shapes with constant thickness of 1.96% of the root chord and 5 to 1 elliptical edges on all sides (Figure 2.1). The two geometries differed only with aspect ratios of 1 and 2. A *Zimmerman* planform is a combination of 2 different sized half ellipses sharing a major axis at a defined longitudinal station. By defining the aspect ratio, root chord and longitudinal location of max span, two half ellipses can be drawn with a shared major axis at the location of max span (Figure 2.2). The two inverse *Zimmerman* planforms chosen for this study have a max span at 75% of the root chord.

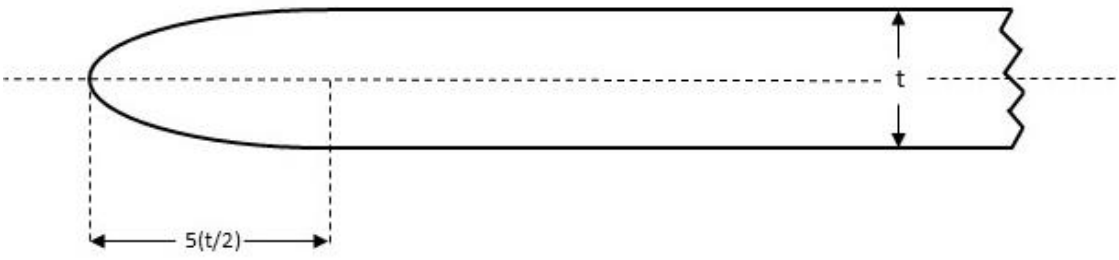

Figure 2.1 An illustration depicting the edge geometry that is found on all side of the wings

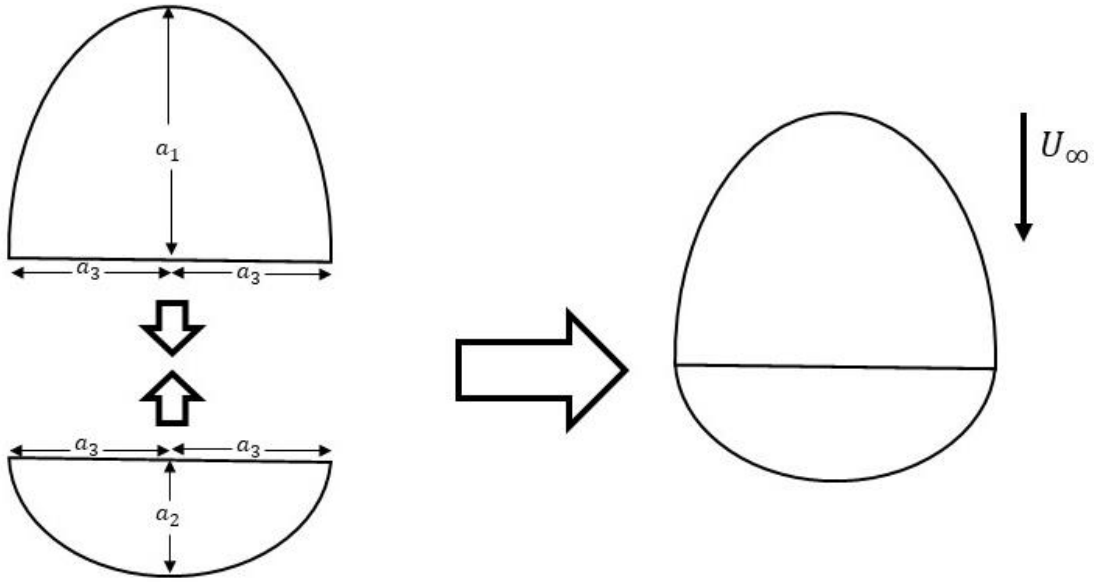

Figure 2.2 A graphical depiction of Inverse *Zimmerman* planform Formation
This depicts an Inverse Zimmerman planform with the max span at the 75% root chord location.

These two geometries were chosen because they both straddle the non-linear lift coefficient increase that occurs at AR below 1.5 (Figure 1.4). Additionally, Mueller recommends this planform over others tested as most tests were observed to achieve the highest lift coefficient. This planform takes advantage of the LEV phenomenon more than other planforms Mueller tested [17]. Keeping in mind that the inspiration for this study comes from a motivation to design a LAR general aviation aircraft, this wing planform shape would fall within a generic shape that might be used as a starting point for design. Ultimately, these geometries were chosen because they represent a reasonable starting point for LAR wing design, they are well documented, and there is high confidence in the reference wind tunnel data.

2.2.2 Physics Continua

Both comparison test cases occur with a Reynold's number off 100,000 based on the root chord; this was matched within the computational analysis. The angle of attack was varied from 10 to 50 degrees with 1 degree increments during the wind tunnel experiment, but the computational analysis will focus on angles greater than zero and no higher than necessary to demonstrate that the stall is not captured by the panel method. Experimental error analysis for comparison data showed near 0% uncertainty at low AoA (< 8-10°) and up to 6% at highest AoA [17]. Using the panel method application strategy being assessed in this study, it is expected that the method will not capture the LEV breakdown and the higher uncertainty is of no significance. Additionally, it was shown that the flow for all tests performed had less than 0.05% turbulence intensity [17]. With the geometry and flow conditions specified generically for both computational methods, the specifics particular to each method will be described next.

2.3 Panel Method Simulations

All panel method solutions were run using a production panel method code named FlightStream. This code implements panel method allowing the user to define Kutta condition and vortex filaments within the flow. Additionally, this code has the ability to include the effect of a boundary layer solution to better capture viscous effect. All flow conditions for the panel method were run with and without the boundary layer solution included to show the effect.

Due to the relatively short solution times obtainable by panel method compared to full finite volume solutions, a 1-degree angle of attack increment was used for both geometries. This allowed for lift coefficient solutions to be compared at every angle that was reported from the corresponding wind tunnel experiment. Additionally, because panel method inherently only requires a surface discretization, the setup of each simulation took significantly less time than the corresponding finite volume solution. All panel method simulations were run using the FlightStream software including the conventional and new application strategy.

To demonstrate the effect of the modified Kutta condition, two of each of the geometries we analyzed with different edges defined with the Kutta condition. Like lift coefficient corrective equations, it would be expected that the modified application strategy of panel method results would

show significantly more lift being produced at higher angles of attack and have better agreement at lower AoA [6][30]. The conventional panel method would not account for the low pressure on the upper surface that occurs due to the LEV and would therefore have a significantly lower lift coefficient estimate (Figure 1.6). In summation, a total of 2 geometries (AR =1 and AR=2) with 2 separate Kutta condition definitions will be run over AoA intervals between 0° to 40° for the AR=1 wing and 0° to 28° for the AR=2 wing to capture the stall. Following subsections will describe the discretization scheme and show grid independence.

2.3.1 Grid Structure

When discretizing, the method takes advantage of wing symmetry and assume that the flow is symmetric across the root chord/center line. This tactic greatly reduces the total number of panels and overall solution time. Solutions are then reflected across the symmetry plane for visual aid during analysis.

The structure uses an aligned quadrilateral mesh from leading and trailing edges to the max thickness contour line (Figure 2.3). Within the max thickness contour, a structured triangular mesh would be used to capture the flat upper and lower surfaces with complementary triangular panels being combined into rectangular panels. The average area and edge length of both types of panels were used to create cells of approximately similar area over the entire geometry. Figure 2.3 also displays the average area of each cell using a color visualization. The relative similarity in color is a good indication that all the panels are roughly the same size. The greatest variance is less than 40% difference in area and is seen where the two discretization types meet. The relative similarities of the area of all panels ease concerns of panels being vastly different sizes causing inaccuracies in results.

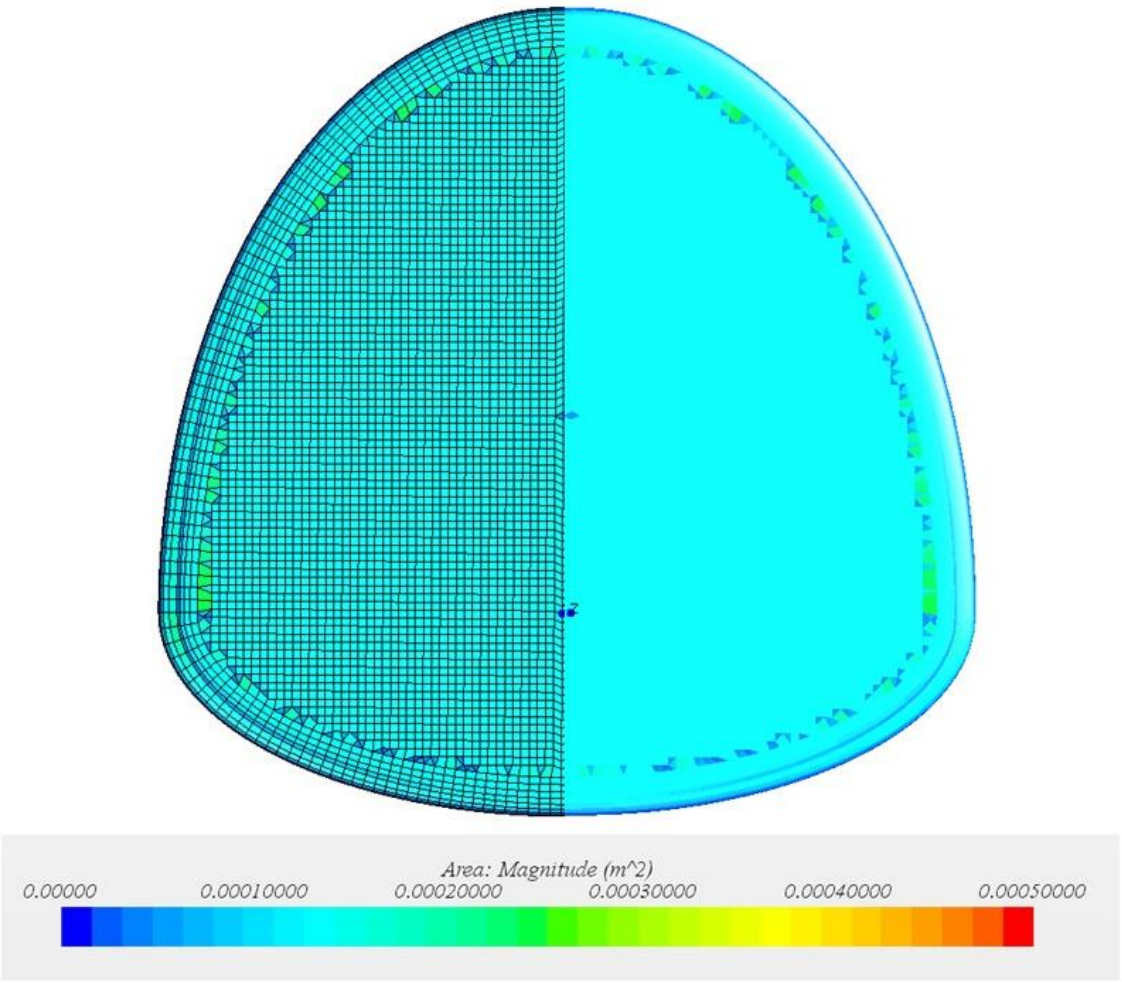

Figure 2.3 Utilized Grid Scheme with Area Visualization.
All edge patches are split into aligned quadrilaterals and the flat portions of the geometry are trimmed structure quadrilaterals. AR = 1 wing shown.

Alternative discretization structures were considered but ultimately this discretization structure chosen for this research. Typically aligned grid meshes offer more solution stability and quicker solutions times [20]. When discretizing the geometry, a structured, trimmed discretization, triangular panels can be combined to result in a majority of the geometry being discretized into quadrilateral panels. This method, over alternatives, also retains the entire wing geometry including all edges. Retaining all edges is a priority because the Kutta condition must be calibrated along the leading edge of the wing and having a portion missing will drastically effect the location of the Kutta condition and resulting LEV. For these reasons, the two geometries were discretized using an aligned quadrilateral grid over the edges and a trimmed, quadrilateral mesh over the flat upper and

lower surface. With discretized geometries, the Kutta condition can be defined along panel edges. The following section presents the methodology for defining these locations.

2.3.2 Kutta Condition Definition

The definition of the Kutta condition along the leading edge has drastic effects on the reported performance and overall flow characteristics around the wings. By changing where this condition is applied, the resulting LEV changes location. Because the LEV accounts for a significant portion of the lift of these wings, the lift coefficient can be changed dramatically with relatively small changes to the Kutta condition location. Therefore, the location where the Kutta condition is defined is critical to the ability of the panel method to accurately capture the lift cause by the LEV.

By defining the Kutta condition further forward on the leading edge, the LEV is shed from a further forward point on the wing. Because it is shed further forward, it travels over more of the wing induces a larger area of lower pressure. Essentially, as the Kutta condition is defined further forward, more lift is produced because the LEV interacts with more of the wings upper surface.

To find the correct Kutta definition location, and essentially calibrate the panel method, the results of the analysis must be compared to other data sources. For this research, the Kutta condition was defined continuously along the leading edge and based on a comparison between the resulting lift curve slope and the experimental force balance data (Figure 2.4). If the resulting lift curve slope was too shallow and needs more lift to match the comparison data, like example (a) in Figure 2.4, the Kutta condition can be defined further forward. Similarly, if the resulting lift curve slope is too steep and reports higher lift values than the comparison data, like example (c) in Figure 2.4, the Kutta condition can be defined further aft along the leading edge.

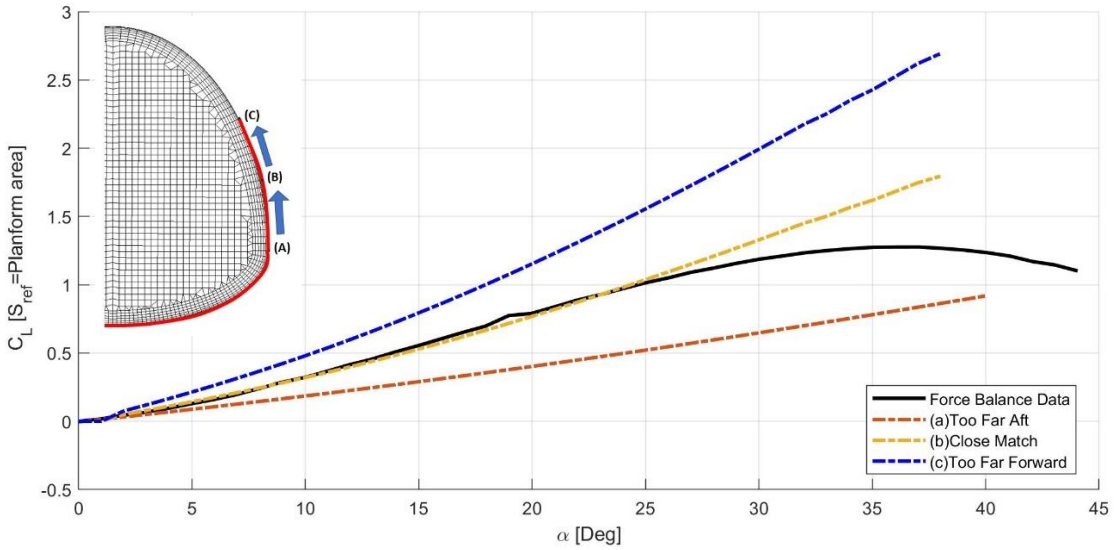

Figure 2.4 Depiction of the Kutta Condition Definition Process for the AR=1 Wing.
The graphic depiction is not to scale with the lift curves seen.

This process of moving the Kutta condition and calibrating where the LEV sheds from requires a comparison data set. Even though this application strategy has been shown to work in capturing the LEV, no documentation could be found to predict the correct Kutta condition locations along the leading edge [23]. This research relied upon existing wind tunnel data sets but using wind tunnel data is not predictive in design applications and does not take advantage of the fast solution times panel method offers. In design applications, comparing to a small set of finite volume solution results can be used to allow for more predictive analysis without having to do wind tunnel tests. This assumes that the finite volume simulations accurately capture the flow field and lift characteristics of the wing being designed. The accuracy of these finite volume simulations, presented later in the results section, is at a level that they can be used to calibrate the Kutta condition definition of the panel methods to capture the lift characteristics of LAR wings.

The final panel method results discussed later in this paper were the final iteration of this Kutta condition definition process. The final locations of the furthest forward point were recorded but do not correspond to where the LEV are observed to shed during wind tunnel experiments[1]. The local sweep angle at this location was 86° and 82° for the AR=1 and AR=2 wings respectively. This corresponded to a half-span location of 97% and 96% and a root chord location of 66% and 70% from the leading edge. This information is summarized below in Table 2.1. These locations

are relatively close to both wings' tips where the freestream flow is perpendicular to the tangent of the edge. The measurements presented in Table 2.1 can be visualized in Figure 2.5

Table 2.1 Final Kutta Condition Definition Locations of Furthest Forward Point

	AR = 1 Inverse Zimmerman	AR = 2 Inverse Zimmerman
Local Sweep	86°	82°
Half Span %	97%	96%
Root Chord %	66%	70%

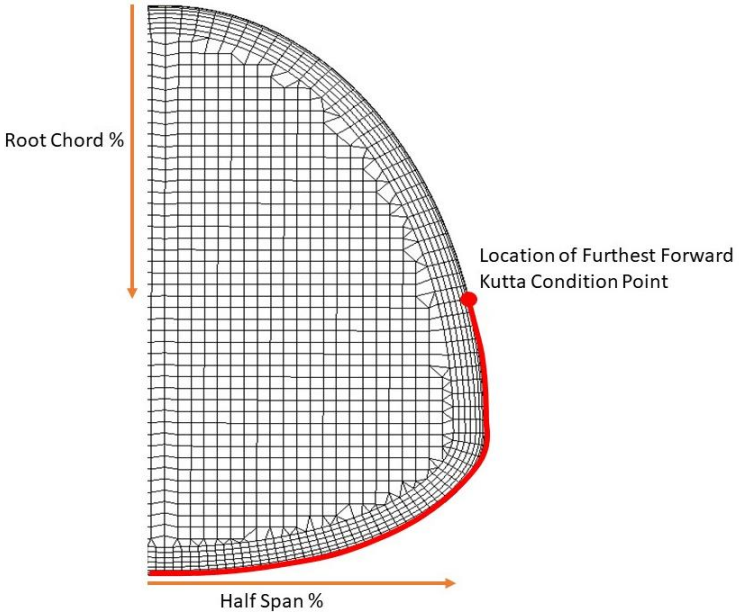

Figure 2.5 A Depiction of Furthest Forward Point of Leading Edge Kutta Condition
Note this is not drawn to scale with the measurements from Table 2.1.

2.3.3 Grid Independence Study

The grid sizing for the panel method analysis was varied by panel area attempting to match the aligned leading edge patches with the structured trimmed mesh average face area. Grid independence was first investigated using an AR 1 wing at 12 degrees AoA to represent a simulation in the middle of the testing sweep. This test point represents a situation where the LEV is well developed and should be a good example of the flow phenomenon inspiring this research Below are the results of the grid independence study investigating the panel method surface mesh used for this research (Figure 2.6). Notice that above 5 thousand panels, the resulting lift coefficient of the wing settles to a value of approximately 0.41. The variance of only 1.1% above 5 thousand

faces inspires confidence that the resulting solution is independent of the discretization scheme. All results from both panel method solutions of the AR =1 wing that are presented in later sections were performed with 10,872 panels.

A similar methodology was performed to show grid independence for the AR = 2 wing with equally as similar results (Figure 2.6). The AoA was set to 8 degrees for this wing as this is within the range of angles which the LEV has influence on the lift characteristics but has not broken down yet. The resulting lift coefficients from this wing settle similarly to the AR=1 wing with grid independence being seen after approximately 5 thousand panels. After 1562 panels, the lift coefficient had a variance of 2.7%. All results from both panel method solutions of the AR =2 wing that are presented in later sections were performed with 10,588 panels.

The small variance in lift coefficient inspires confidence in the fact that the results from the panel methods should be independent of the discretization. As a result, differences seen between panel method results and other data sources cannot be due to the discretization of the wings being too course.

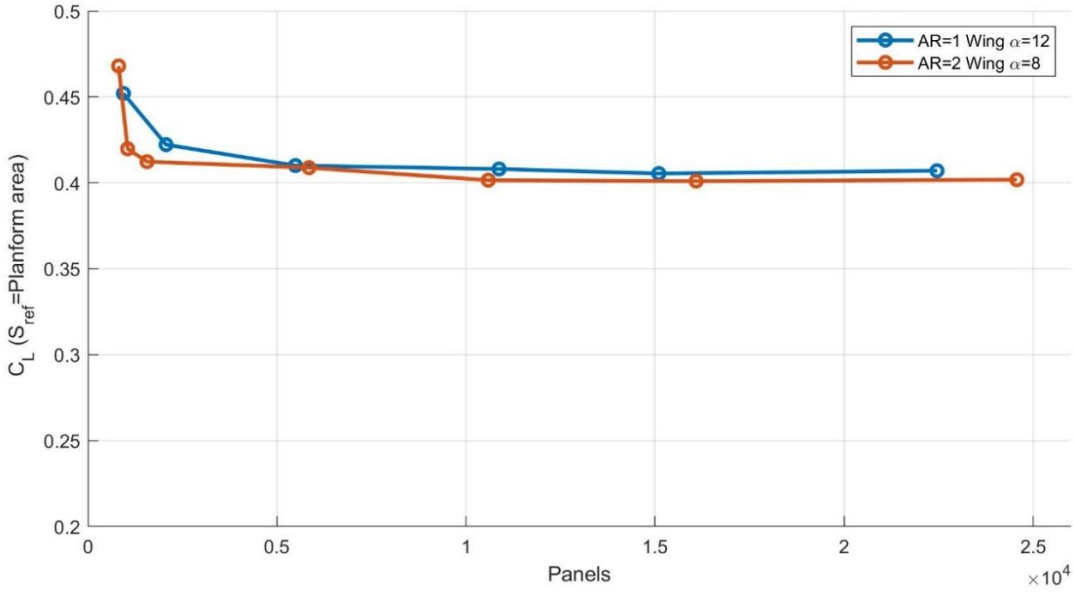

Figure 2.6 A Comparison Between C_L and Number of Panels.

2.4 Finite Volume Simulations

Due to the increased setup and run time required for a finite volume solution, the two geometries were analyzed at 4° increments from 0° to 40° for the AR=1 wing and 0° to 28° for the

AR=2 wing. This is meant to include region of the lift curve influenced by suction lift as well as the gentle stall associated to the breakdown of the LEV. Unlike the panel method solutions, the finite volume solution would be expected to accurately capture the breakdown of the LEV and report lower lift coefficients after the LEV breakdown. This would demonstrate the higher fidelity attained as well as the higher computational cost.

The following section documents the setup and inputs into the finite volume solutions used to generate the results discussed in later sections. It should be noted that although the finite volume solution was very predictive in contrast to the modified application strategy of panel method describe in the previous section, the simulations required significantly more inputs and setup. All finite volume simulations were run using StarCCM+ v.2020.1.

2.4.1 Physics Continua

To solve this steady flow phenomenon, RANS equations were used with a segregated flow solver. A segregated flow solver solves each of the momentum equations in turn while a coupled flow solver solves momentum, energy, and mass simultaneously. A coupled flow solver typically has advantages when solving for a flow field with compressibility effects but offers no advantage for this research purpose. Additionally, the flow was solved as incompressible. This assumption is reasonable for the Mach number associated with this analysis. Finally, the turbulence was modelled using the realizable κ-ε equations which is recommended for separation and boundary layer prediction. Ultimately, because the LEV is a potential flow driven phenomenon, the choice of turbulence model was assumed to have little effect on the results.

The free stream boundary conditions were set based on the standard atmosphere model at sea level and is outlined in the Table below. The freestream velocity was set to match the Reynold number of the experimental data using typical air viscosity and a root chord length of 1 meter for both wings. Therefore, the freestream velocity is 1.47 m/s (3.15 mph). All physical condition input parameters are summarized in Table 2.2.

Table 2.2 Input Parameters for Finite Volume Solutions

Input Parameter	Value
$P_{atmosphere}$	101.325 kPa
$T_{atmosphere}$	15° C
$\rho_{atmosphere}$	1.225 kg/m^3
Re	100,000
μ_{air}	1.81 × 10^{-5} kg/(m·s)
V_∞	1.47 m/s

2.4.2 Grid Structure

The fluid domain was set as a hemisphere with radius 30 times the root chord length; this was assumed to be large in all directions to achieve accurate results. At that hemisphere surface, the freestream conditions were applied while a symmetry condition was applied at the plane of the wing root. This fluid domain was assumed to be symmetric about the root plane of the wing allowing for significantly reduced computational time.

The solution domain was discretized using a polyhedral mesh scheme with an additional prism layer near the surface of the wing geometry. All results discussed later used a polyhedral mesh growth rate of 1.1 with a max size limited by the longest edge length being 15% of the root chord length. The prism layers were sized using a y+ wall growth with y+ set to 1 which was recommended when using the κ-ε turbulence model, where u_* represents friction velocity.

The total height of the boundary layer was determined using the Blasius solution for an infinitely long flat plate (equation 2.1). The first cell height from the wall is determined using a friction coefficient estimation based on a flat plate. The complete calculation is described in a referenced boundary layer and viscous flow textbook [30].

$$\delta = \frac{5.0x}{\sqrt{Re}} \tag{2.1}$$

In practice, the amount of prism layers is limited to decrease runtime as these layers can constitute a majority of the total cell count. For this research, it was decided that it was better to err on the side of having too many prism layers as the computational time for solving is not a limiting factor.

2.4.3 Grid Independence Study

The mesh sizing for these simulations focused on the field mesh above the wing in an attempt to capture the LEV flow feature. For simplicity, the prism layer remained the same because

the LEV occurs above the boundary layer above the wing and the field polyhedral mesh was constrained using growth rate and target size. Grid independence was investigated using an AR=1 wing at 20 degrees AoA to represent a simulation in the middle of the testing sweep. This test point represents a situation where the LEV is well developed and should be a good example of the flow phenomenon inspiring this research.

Below are the results of the grid independence study investigating the finite volume solution grid used for this research (Figure 2.7). Notice that above 3 million cells, the resulting lift coefficient of the wing plateaus to a value of approximately 0.388. The relatively tight variance of only 0.4% above 2.7 million cells inspires confidence that the resulting solution is independent of the discretization scheme. All results from finite volume solutions presented in later sections were performed with 6.95 million as the total solution times were not vastly different than those run with ~3 million cells. In practice, this grid scheme should be run with the lowest cell count possible to remain grid independent; this occurs above 3 million cells.

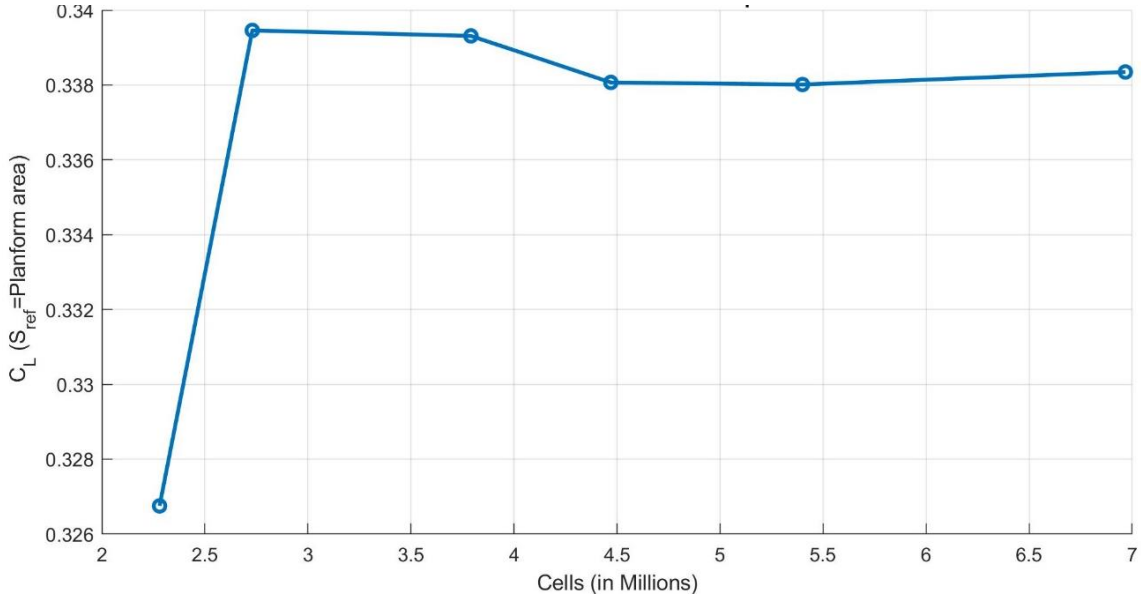

Figure 2.7 Comparison between C_L and Number of Cells.

2.4.4 Trefftz Plane

To provide validation for the induced drag calculations from the modified application of panel method, the finite volume analysis must be used because the reference wind tunnel data did not separate the drag. Total drag from both computational methods will be compared with the

reference experimental data while the induced drag will only be compared between the computational methods. By comparing the induced drag only, the effect of the skin friction calculation within FlightStream can be observed. To obtain the induced drag from the StarCCM+ simulation, a *Trefftz* plane can be used.

A *Trefftz* plane is a surface integral of a plane within the wake of a geometry that is used to calculate the induced drag force produced on the geometry [23]. Equation 2.2 presents the surface integral that is calculated where ρ_∞ represents the freestream density and D_i represents induced drag force. Note that this sums the velocity components (v and w) that are not in the freestream direction. Additionally, the plane must be placed far enough away from the geometry within the wake that the final reported value has reached an asymptotic value. Having the plane placed too close will typically overestimate the induced drag force. In this study, it was found that this location must be greater than 6 chord lengths away to reach the true value. The results of the induced drag comparison will be presented and discussed in the following chapter.

$$D_i = \frac{1}{2}\rho_\infty \iint_S (v^2 + w^2)dydz \tag{2.2}$$

3. RESULTS

This chapter presents the results of running the simulations described in the methodology sections. The results include a comparison of the lift and drag coefficients resulting from the two CFD analyses and the corresponding wind tunnel experiment. This will provide an avenue for validation of the finite volume solutions and demonstrate the new application strategy for panel method accurately modelling the LEV and resulting suction lift. After validating the finite volume resultant forces, the pressure distribution resulting from the two CFD methods are compared. The higher confidence in the finite volume solutions allows for further comparison to the panel method results to assess pressure distributions and flow features.

3.1 Lift Comparison

When plotting the lift coefficient versus the AoA, there is good agreement between the finite volume solution and experimental data in all simulations, see Figure 3.1 and Figure 3.2. The variance between these two data sources was less than 8% of the C_L at all AoAs and less than 6.5% before the stall. It would be expected that the finite volume analysis and experimental data would agree more strongly at lower AoAs as the flow is much steadier and there is less uncertainty in experimental data. Referring to the original paper, the uncertainty of the data points at higher AoAs is greater than the difference between the reported value and the finite volume analysis [17]. It can be said that the finite volume analysis accurately models the lift characteristics for both wings.

When including the results from both the conventional panel method and the alternative application strategy, there is a reasonable agreement between the new application strategy of panel method analysis, finite volume analysis, and experimental data before LEV breakdown and, as expected, the conventional panel method fails to model either wing's lift characteristics (Figure 3.1)(Figure 3.2). As expected, because the conventional panel method analysis does not account for the lift caused by the LEV the resulting lift coefficient is significantly lower than all other data sets. This disagreement increases as the effect of the LEV becomes more dominant. As expected, neither the panel methods capture the stall phenomenon and the lift coefficient continues to grow with AoA. The new panel method application strategy shows good agreement with the finite volume analysis and experimental data before the LEV breakdown and stall. For the AR=1 wing, the

modified application strategy panel method results differed from experimental data less than 6.8% before 25 degrees AoA; this corresponds to a lift coefficient of 1. For the AR=2 wing, this error was slightly more at 9.6% before 12 degrees AoA, but there was increased uncertainty in the experimental data as well. After these AoAs, there is little agreement between either panel method and the experimental data. Again, this is expected because these methods do not account for the breakdown in LEV and loss of lift. Overall, the modified application strategy of panel method captures the non-linear lift associated with the formation of a LEV and because it doesn't account for stall or LEV breakdown, it is no longer accurate at AoAs above the stall point.

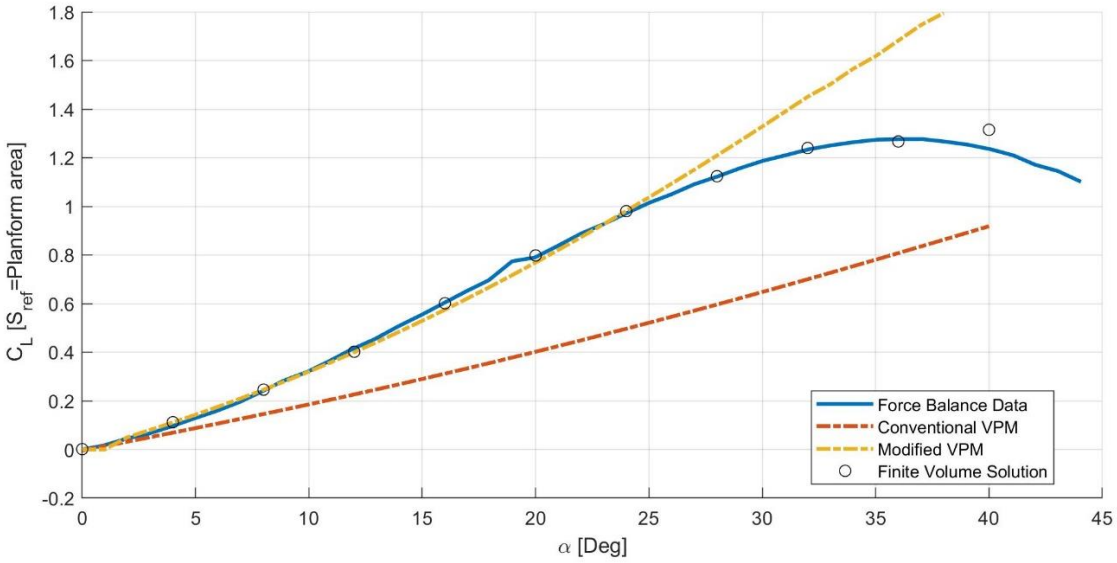

Figure 3.1 C_L vs α from Both CFD Methods and Experimental Data for AR = 1

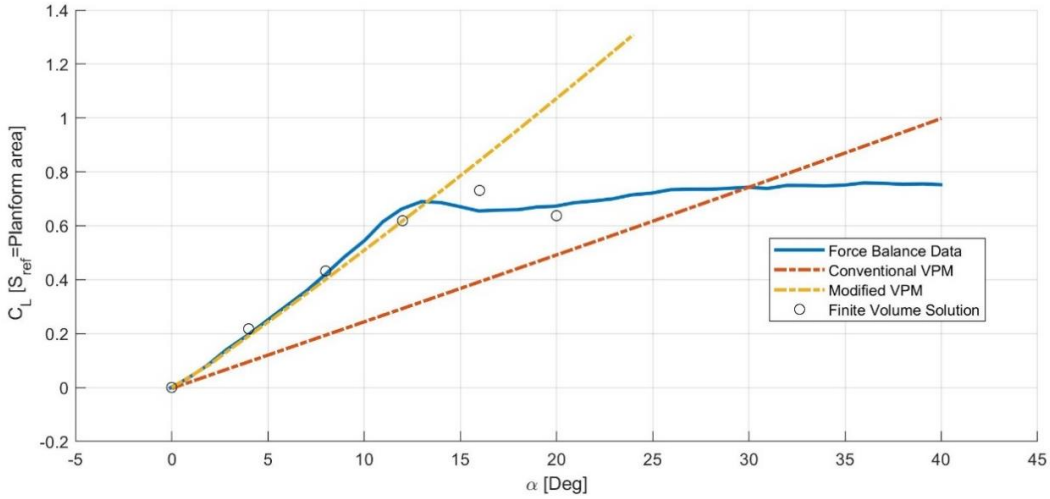

Figure 3.2 C_L vs α from Both CFD Methods and Experimental Data for AR = 2

It is important to keep in mind that even though the modified application of panel method can capture the non-linear lift associated to the LEV, the methods presented in this paper are not predictive if analyzing a novel wing design. The lift curve slope of the reference experimental data was used to determine how much of the leading edge should have the Kutta condition applied to it. Essentially, without an initial calibration and comparison of the panel method, there is a small chance of achieving usable results. This is a current limitation in the ability to apply this method to design applications. In contrast, all finite volume solutions were run as a predictive tool that captures the flow without comparison to experimental references. In an application to design a LAR wing, finite volume solutions can be used as a method to predict the lift characteristics of that wing.

3.2 Drag Comparison

Because potential flow analysis can only provide induced drag predictions, it is important to verify the level of accuracy of the panel method predictions without the built in FlightStream boundary layer solver. First the induced drag results from all CFD methods will be discussed. This is followed by a presentation of total drag estimations from all CFD methods and the wind tunnel force balance data. Overall, the modified application strategy of panel method showed good agreement with induced and total drag estimations with all comparison data sets.

3.2.1 Induced Drag

Overall, the induced drag predictions showed good agreement between the modified application strategy of panel method and the StarCCM+ finite volume solutions (Figure 3.3)(Figure 3.4). These two computational methods show discrepancies at increased AoA. Of course, it is not expected that either panel method would match with any other data set at AoAs beyond where the wing has stalled. This occurs at 20° for the AR=1 wing and 12° for the AR=2 wing. Beyond this stall point, the modified application strategy of panel method induced drag predictions have increased difference from the finite volume results, but match better than the conventional application method results at all AoA. The good agreement between the modified application strategy of panel method and finite volume predictions of induced drag inspire confidence that this modified application

strategy of panel method have the potential for modelling the induced drag characteristics of LAR wings.

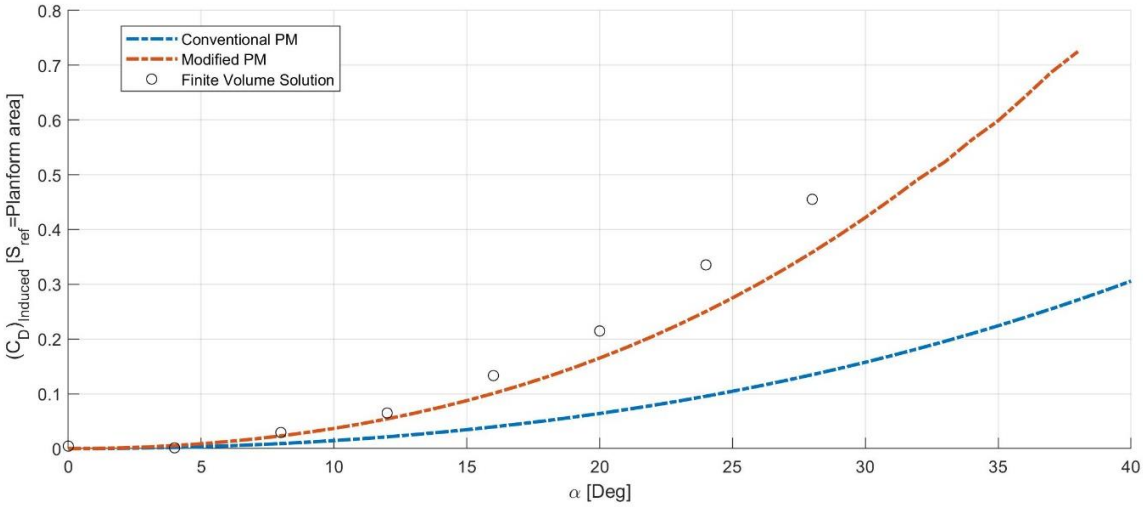

Figure 3.3 $(C_D)_{Induced}$ vs α from Both CFD Methods and Experimental Data for AR = 1 Wing

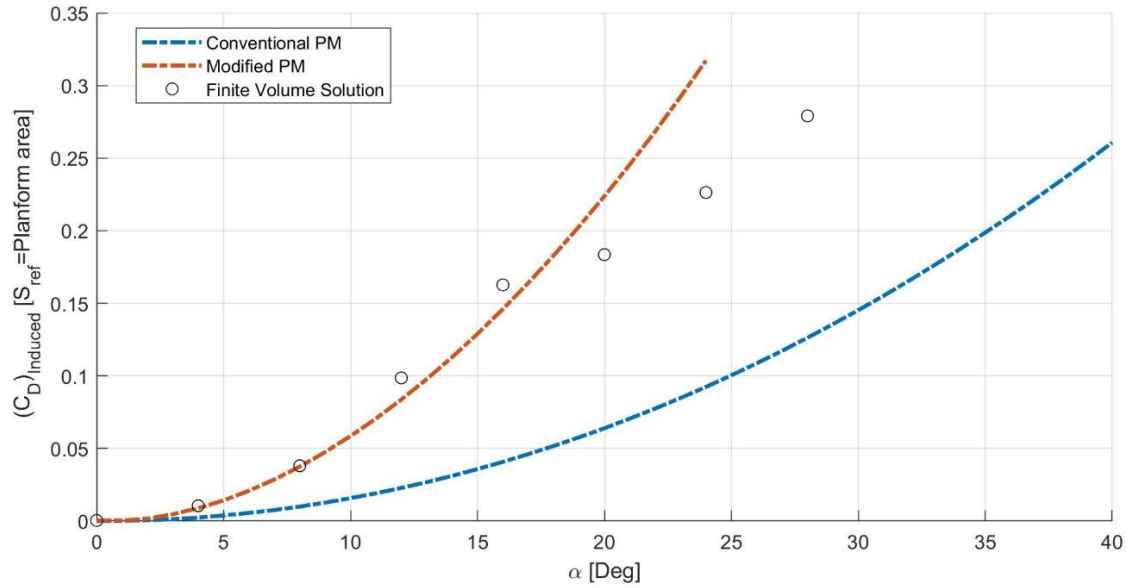

Figure 3.4 $(C_D)_{Induced}$ vs α from Both CFD Methods and Experimental Data for AR = 2 Wing

3.2.2 Total Drag

Upon examination of the total drag results there are some key things to take away. All CFD results underestimate the total drag coefficient when compared to the experimental data and the modified application strategy of panel method captures the drag characteristics of the wings better than the conventional panel method.

Overall, the finite volume analysis was able to estimate the drag fairly well with better accuracy when applied to the wing of AR=1. For the AR=1 wing, the finite volume drag prediction was within 3.2% error compared to the experimental data. For the AR = 2, the total drag estimation was significantly less accurate with the largest error being ~30% when compared to the wind tunnel results. It is important to note that the accuracy of the AR=2 finite volume analysis was significantly better before the wing stall indicating that the turbulent, separated flow after stall was not captured correctly by the simulation. Typically, it would be expected that the finite volume analysis would underestimate the drag force on the wing.

When examining the panel method results, it is apparent that because the modified panel method application strategy captures the induced drag characteristics of both wings significantly better than the conventional panel method it also captures the total drag characteristics better as well. The modified results are closer to experimental results at all AoAs. This was expected because a significant portion of drag for LAR wings at high AoA is produced by lift as induced drag. Because the modified application strategy of panel method captures the additional lift caused by the LEV, it also captures the additional induced drag caused by the LEV. Just like the finite volume solutions, all drag predictions from both panel method estimations are underestimates.

The inclusion of the boundary layer approximation for the panel methods made the drag predictions more accurate than the induced drag predictions alone. Upon comparison to the panel method simulations without the boundary layer approximation it is revealed that FlightStream applies a constant viscous drag force value regardless of AoA. Regardless of this method's simplicity, this simple calculation makes the both the conventional and modified application strategies of panel method more accurate when predicting total drag. In practice a more sophisticated viscous drag estimation method can be applied with the inviscid panel method analysis for more accurate estimations of drag characteristics. Overall, the modified application strategy, with the boundary layer estimation, has shown the potential to accurately capture the total drag characteristics of LAR wings.

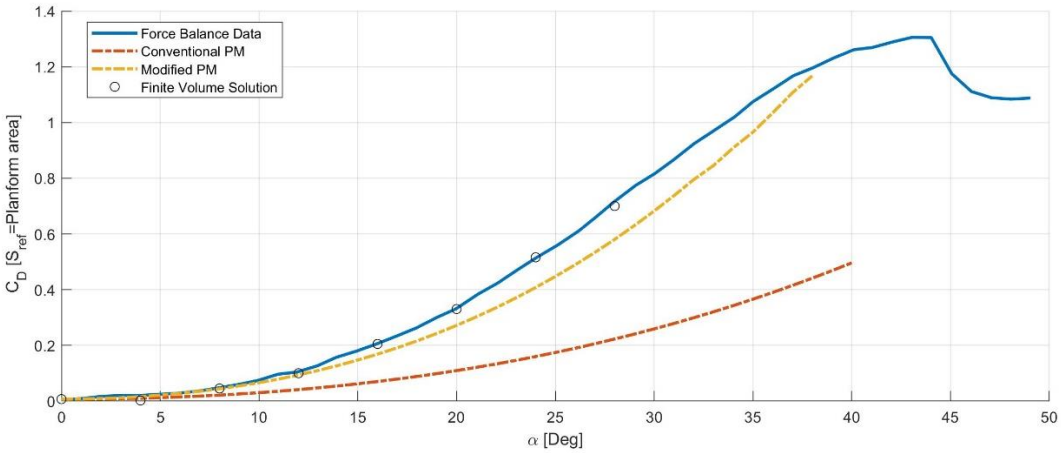

Figure 3.5 C_D vs α from Both CFD Methods and Experimental Data for AR = 1 Wing

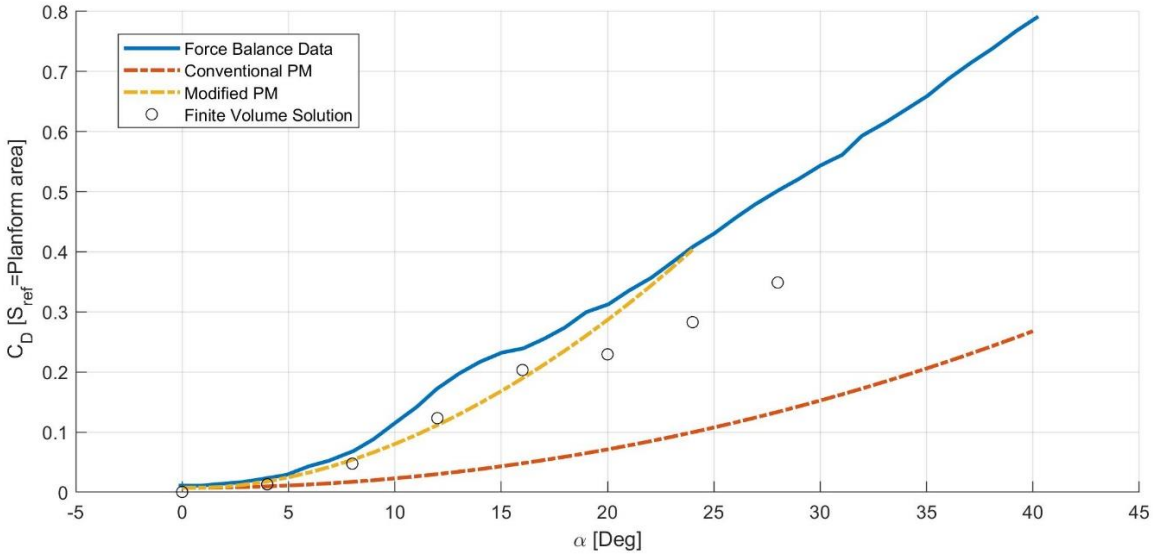

Figure 3.6 C_D vs α from Both CFD Methods and Experimental Data for AR = 2 Wing

3.3 Moment Comparison

An important characteristic for the design of a wing is the moment coefficient characteristics over a range of AoAs. For tailless aircraft, like many low aspect ratio aircraft, the accurate prediction of these qualities is integral to the longitudinal stability of the final aircraft. Figure 3.5 and 3.6 show the C_M versus AoA for both wings with results from all analysis techniques. All moment coefficients are referenced about the quarter root chord location.

Additionally, it is important to keep in mind where the panel methods are accurate. Beyond stall, both panel methods no longer agree with experimental results. From this, it is expected that the moment coefficients would not agree with experimental comparison or finite volume results.

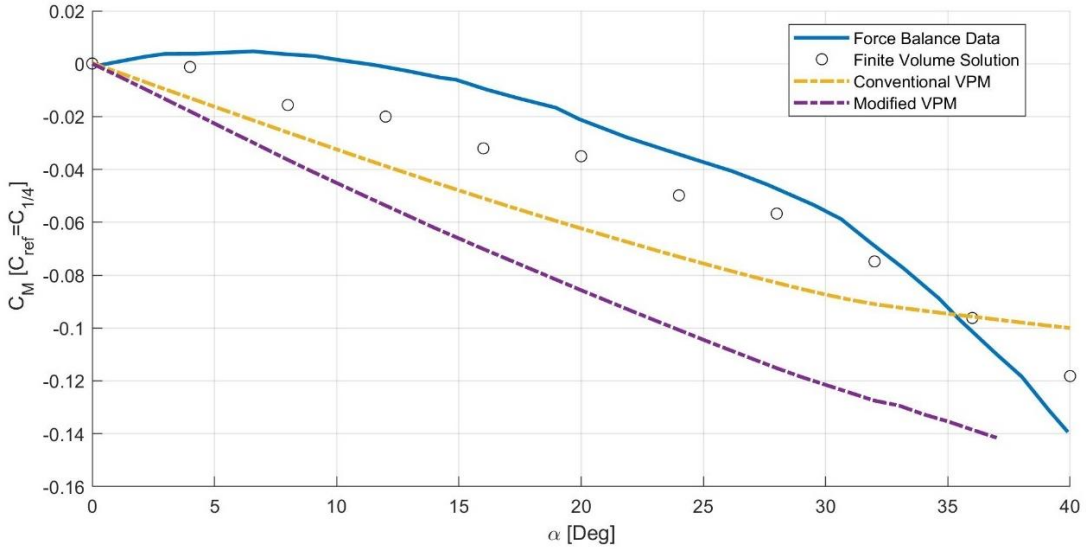

Figure 3.7 C_M vs α from Both CFD Methods and Experimental Data for AR = 1 Wing

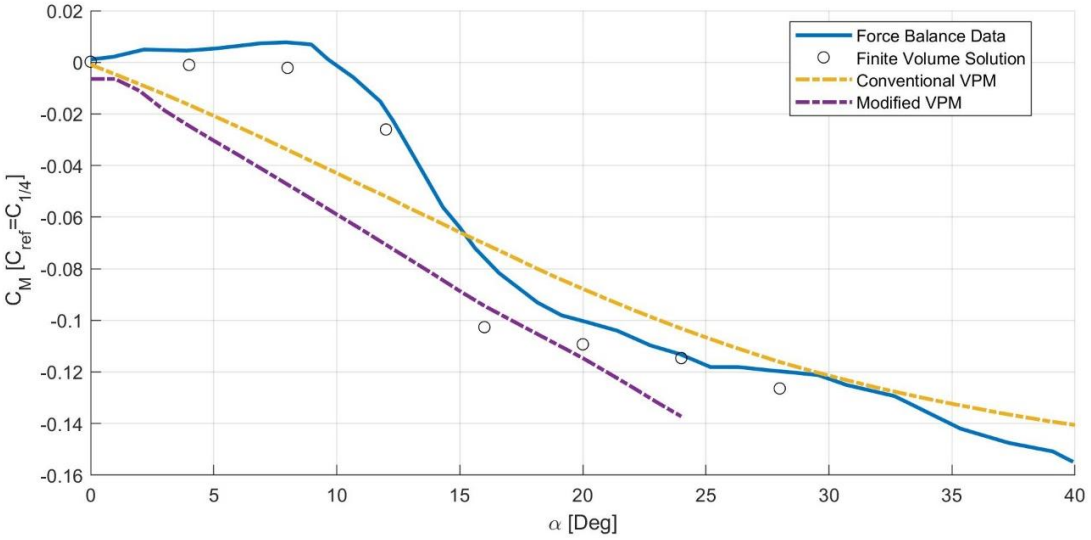

Figure 3.8 C_M vs α from Both CFD Methods and Experimental Data for AR = 2 Wing

The finite volume solution results for C_M have the closest match to the experimental data sets. The finite volume analysis predicted the general trends for both wings with relatively good accuracy, especially considering the vastly different behavior seen between the two wings. When referencing the original paper, the moment coefficients recorded had an experimental uncertainty

of 10% at all angles. The finite volume C_M for the AR=2 wing falls within this uncertainty but lie slightly outside of this uncertainty for the AR=1 wing. Overall, the finite volume simulations yielded moment coefficients that estimate the behavior of the true wings well with some variation from experimental results.

When examining the resulting moment coefficients from the 2 panel methods, the estimation is significantly less accurate than the finite volume results. Both the conventional and modified panel methods predicted a negative relation between C_M and AoA which overall is the final trend for both wings, but these methods both failed to match the inflection seen in the experimental results. In all cases, however, the modified panel method had better estimations of the moment coefficient when compared to the conventional panel method results.

All computational method failed to predict the initially positive moment coefficient that was seen in the experimental results. The finite volume results for the AR=2 wing come close with a nearly flat portion of the curve at low AoA and then capturing the inflection to significantly more negative moment coefficients around the stall point. The discrepancies between the reported moment coefficients from the different computational methods indicate that there will be significant discrepancies in the pressure coefficient distributions over the wing. This is discussed further in the following section.

3.4 Pressure Distribution Comparison

With the higher confidence in the finite volume solutions, the results can be used as a good representation of the actual time-averaged flow field. By comparing the results from the modified application strategy of panel method simulations to the finite volume simulation results, conclusions can be made about the ability of the panel method to capture the flow field around the wing. Pressure coefficient was used to visualize the LEV effect on the upper surface for both simulations. As predicted by variation between moment coefficient predictions, the pressure distributions over the wings have significant discrepancies. This section presents general trends and observations about pressure distributions and identifies discrepancies between the analysis techniques. Only modified panel method results are presented in this section as the results have shown reasonable agreement to experimental and finite volume results for lift and drag coefficient.

3.4.1 Lower Surface

The lower surface shows good agreement at lower angles of attack on both wings between the finite volume solutions and the modified application strategy of panel method solutions. As the AoA increases, higher pressure (visualized by warmer colors) is seen at the leading edge with focus in the center; this trend continues past the breakdown of the LEV and stall because the lower surface is not influenced as strongly be these phenomena (Figure 3.7)(Figure 3.8). These trends are observed in both the AR=1 and AR=2 wings.

A disagreement is observed at higher AoA and can be visualized as the region of higher pressure (red) growing further back and outward in the modified application strategy solutions. This raises concerns about the modified application strategy's ability to capture the true flow field. There is an additional concern when observing the modified application strategy as a thin region of low pressure is seen at the leading edge (visualized with a blue band). This disagreement is an important note as it most likely contributes to the disagreement in predicted moment coefficient. The increased high pressure at the trailing edge and low pressure at the leading edge on the bottom surface of the wing would contribute to a more negative moment coefficient.

These disagreements become stronger at higher angles of attack. This is expected because the lift coefficients above 20°for the AR=1 wing and above 12° for the AR=2 do not agree with the experimental results of finite volume results. It would be expected that the pressure distributions would only agree in the AoA regime where the coefficient of lift agrees.

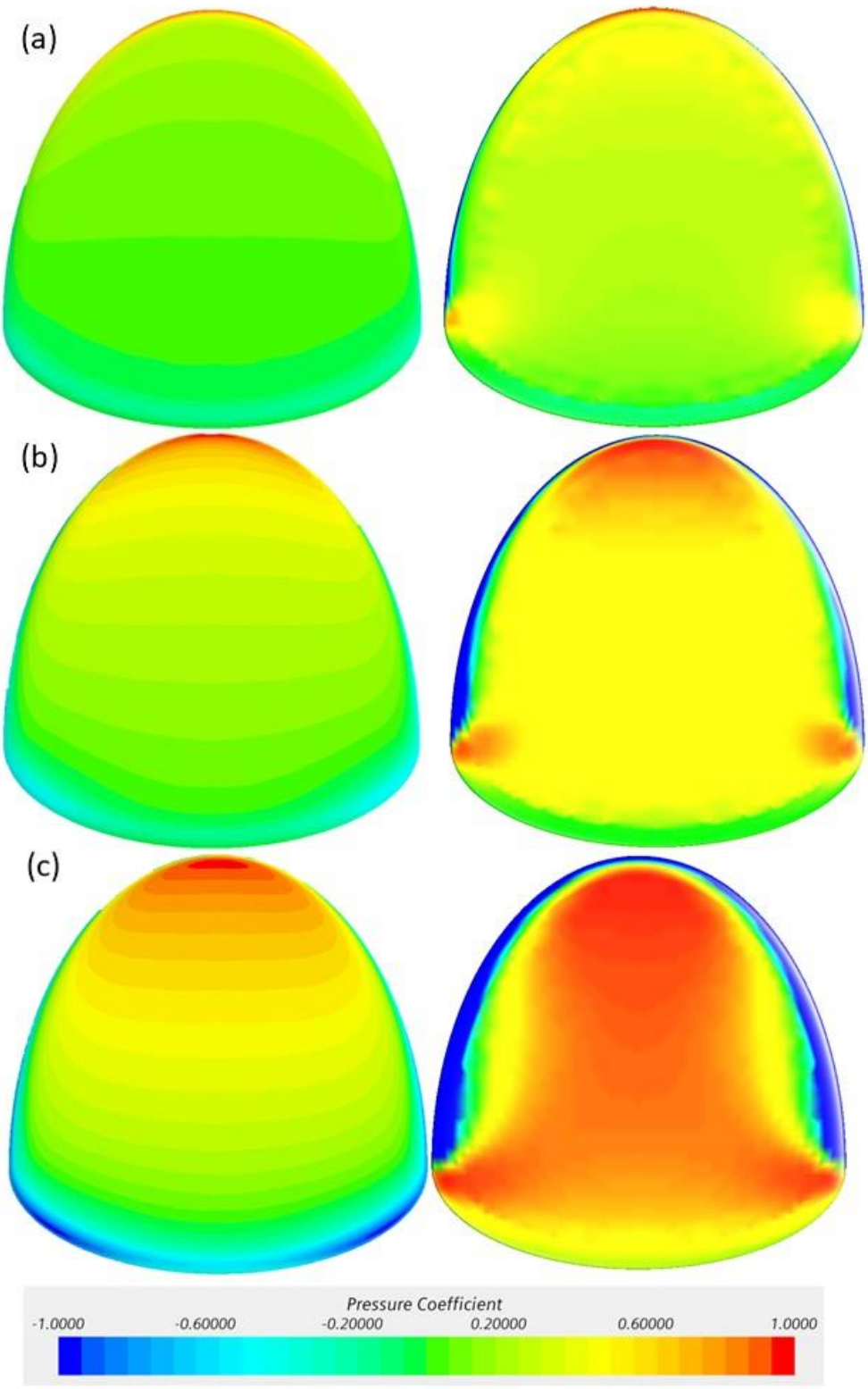

Figure 3.9 Lower Surface C_P distributions of AR=1 wings for various α
Finite volume solutions on the left and modified application strategy solutions on the right
(a) $\alpha = 4°$ *(b)* $\alpha = 20°$ *(c)* $\alpha = 36°$

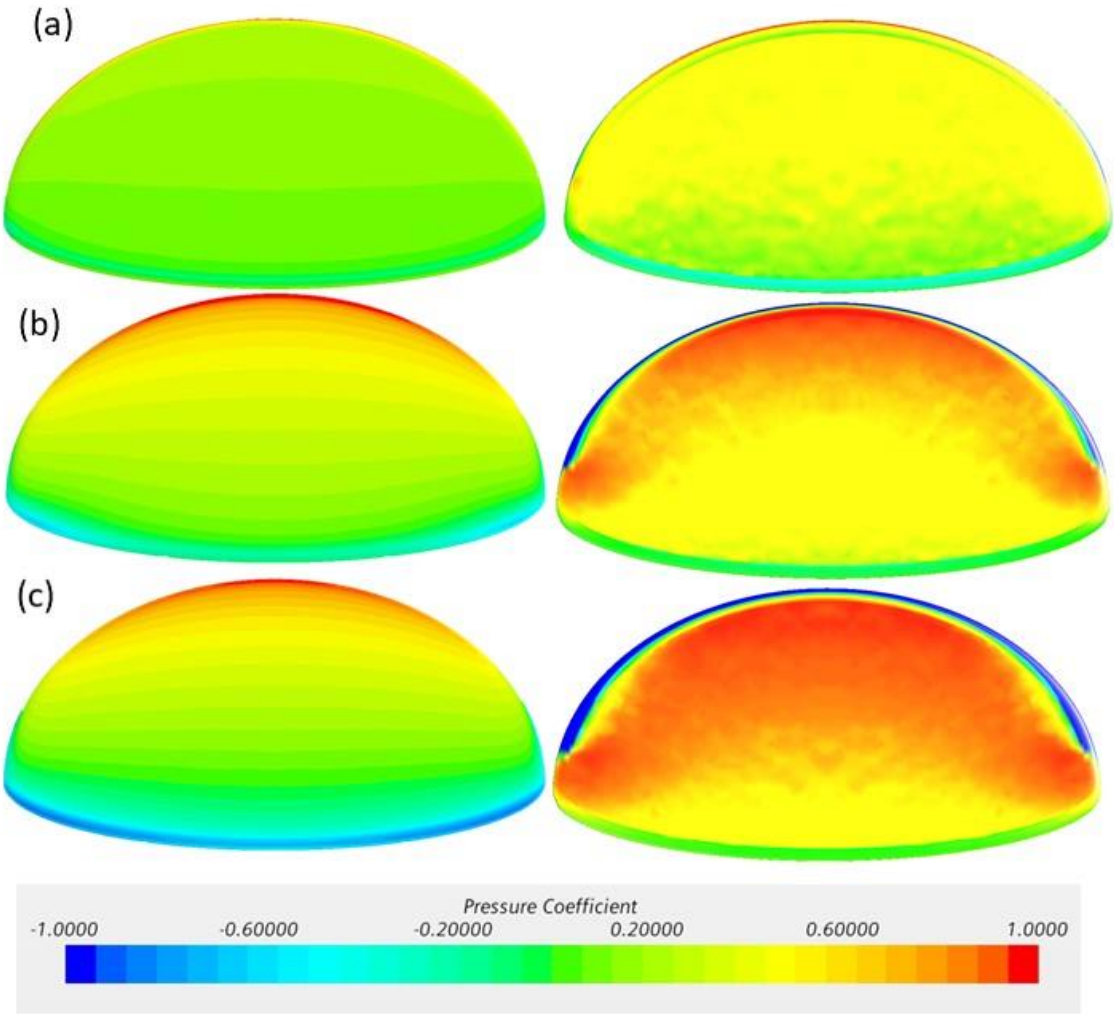

Figure 3.10 Lower Surface C_P distributions of AR=2 for various α

Finite volume solutions on the left and modified application strategy solutions on the right; (a) $\alpha = 4°$ (b) $\alpha = 16°$ (c) $\alpha = 24°$

3.4.2 Upper Surface

The upper surface pressure coefficient distributions define the whole purpose of this paper by allowing for visualization of the LEV. There is good agreement between the finite volume and modified application strategy solutions at lower AoA. Figures 3.9 and 3.10 depict the LEV locations on the two wing geometries through a region of low pressure (blue) emanating from the leading edge and trailing aft. Both the finite volume and modified application strategy predict a thin strip of low pressure at the leading edge at low AoA. As the angle is increased, this region grows wider. This agreement shows that a modified application strategy has the ability to capture the LEV phenomenon. As the angle is increased, the finite volume solution indicates that the LEV is shed from an increasingly further forward location on the leading edge. Because the panel method used the same Kutta condition at all AoA, the LEV was shed from the same location throughout and the LEV grew stronger.

As the AoA is increased further, the finite volume solutions capture the stall and LEV breakdown which is visualized by a large (nearly isobaric) low pressure zone behind the wing. The panel method does not account for this phenomenon and the LEV continues to grow stronger past the point where the LEV has broken down and the wing stalls. This is expected and would be kept in mind in design applications of a modified application strategy.

Additional observations can be made of the flows over either wing and compared using the finite volume results to understand how AR can effect the formation of a LEV. On both wings, as the AoA is increased, the LEV can be observed to get stronger (visualized by a wider region of low pressure) and sheds from a further forward location. Regardless of this, the LEV attempts to flow backward just inside the leading edge which most likely due to the low pressures at the leading edge and the resulting spanwise flow that is characteristic of swept leading edge wings. Additionally, when comparing between the two wings, it can be observed that the LEV breaks down in a similar fashion for both wings; after the stall, the entire upper surface is nearly all the same low pressure.

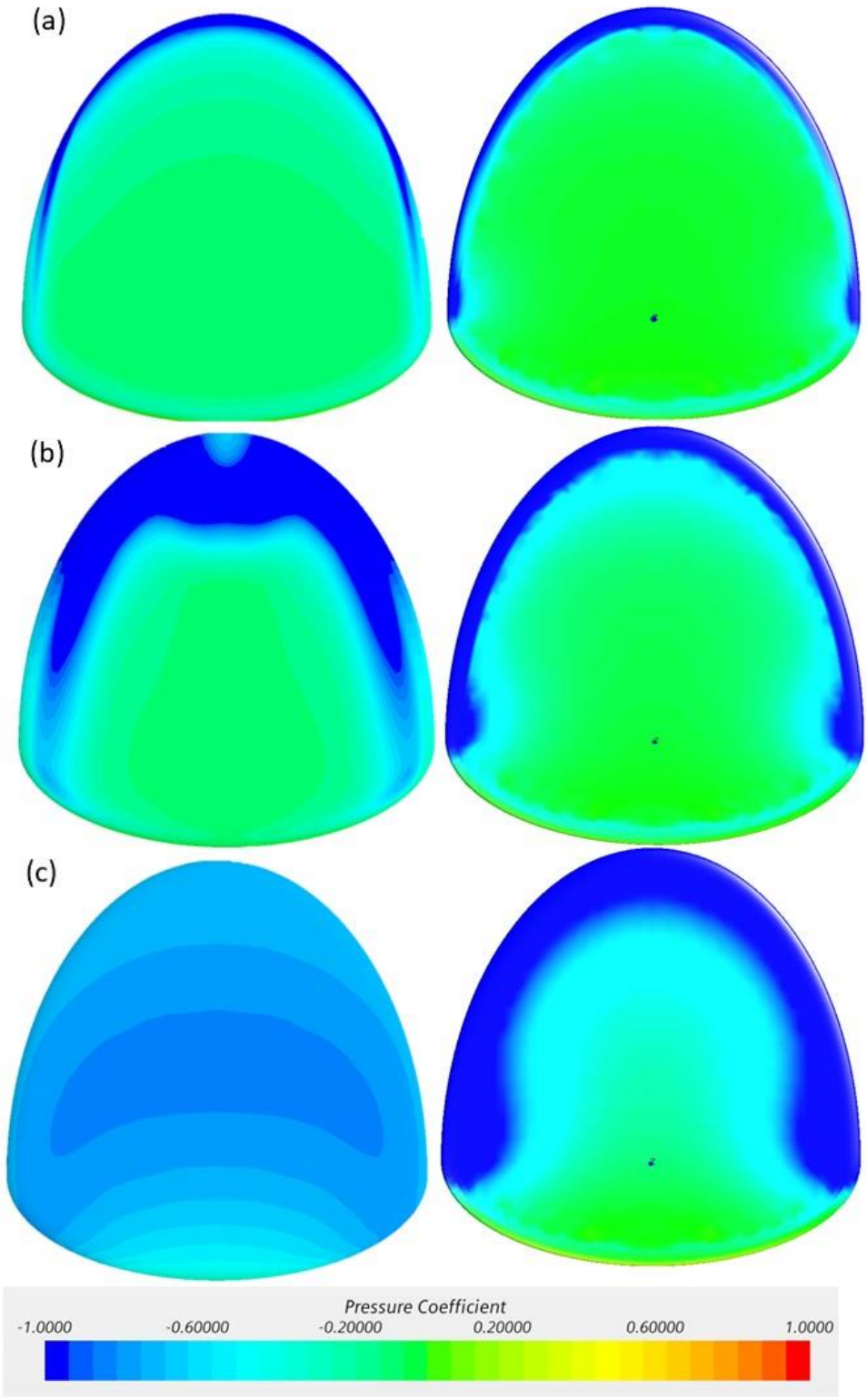

Figure 3.11 Upper Surface C_P distributions of AR=1 wings for various α
Finite volume solutions on the left and modified application strategy solutions on the right
(a) $\alpha = 8°$ *(b)* $\alpha = 16°$ *(c)* $\alpha = 32°$

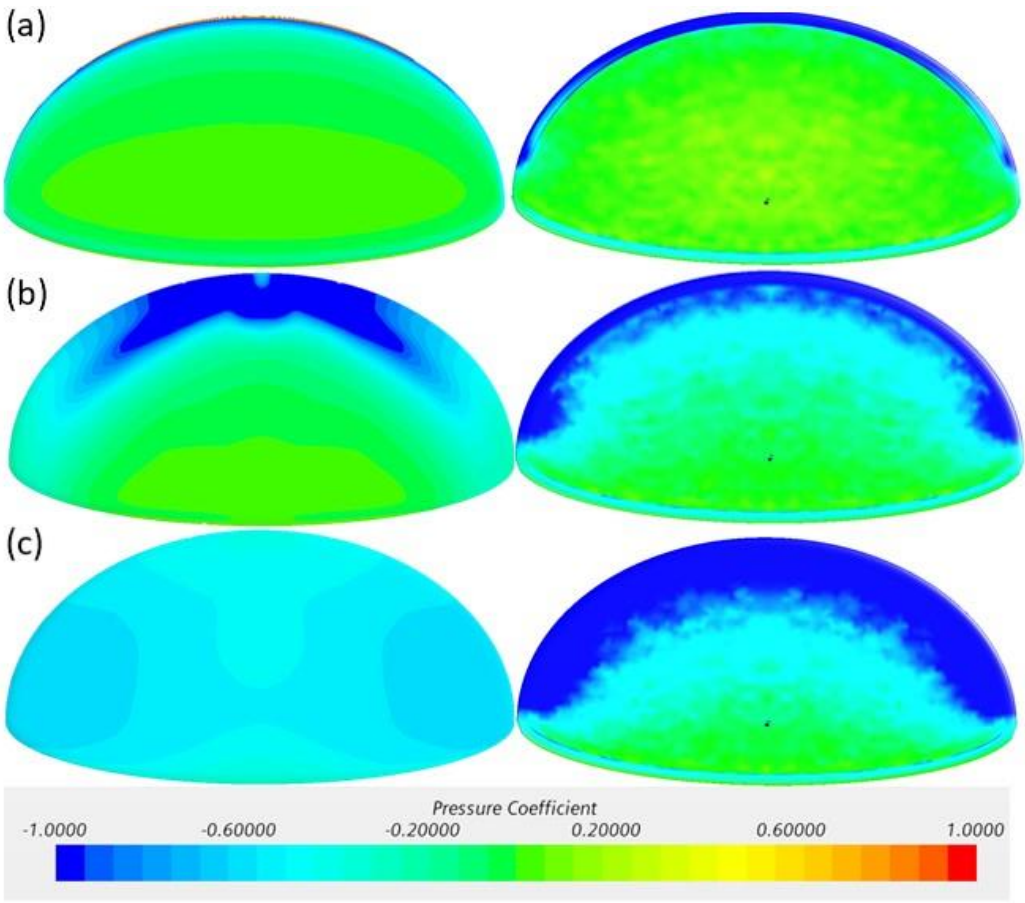

Figure 3.12 Upper Surface C_P distributions of AR=2 wings for various α
Finite volume solutions on the left and modified application strategy solutions on the right
(a) $\alpha = 4°$*(b)* $\alpha = 12°$ *(c)* $\alpha = 20°$

3.5 Solution Time Comparison

At this point, it may seem attractive to use finite volume analysis for all design work involving the applications of LAR wings as it can accurately predict flow characteristics. However, the time it takes to yield a result would be a huge limitation at early design phases when the design changes quite often. Table 3.1 presents the solution time for 1 AoA on each wing. The solver was stopped after all residuals fell below 1e-4. These solution times are a small sample of all solutions run but represent the magnitude of the difference in solution times. Earlier in the design phase, the higher fidelity/accuracy that a finite volume solution offers may not be worth the time it takes to generate results. Additionally, at early design phases, the level of detail of the design does not merit the level of fidelity that finite volume solutions offer. To analyze the same wing, it could take the finite volume solver 20-30 times longer than the panel method solver.

All solutions for all CFD simulations were run on a desktop machine with a 2.6 GHz Intel Xeon processor. It was an 8-core machine with 64 GB of RAM and a Quadro 5000 graphics coprocessor. Because all simulations were run on the same machine, rough comparisons of solution times can be made between both solution methods. It is important to keep in mind that each solution application utilizes available memory and processing in different ways, but the relative difference in magnitudes between solution times makes this an insignificant issue since they were run on the same machine.

Table 3.1 Comparison of Solution Times for a single α

Solution Type	Solution Time
Panel Method - AR1 - $\boldsymbol{\alpha = 12}$°	23 min
Panel Method - AR2 - $\boldsymbol{\alpha = 8}$°	18 min
Finite Volume - AR1 - $\boldsymbol{\alpha = 12}$°	10 hrs 43 min
Finite Volume - AR2 - $\boldsymbol{\alpha = 8}$°	8 hrs 26 min

It is also important to understand that the setup of the finite volume solvers took significantly longer than the panel method. Table 3.1 only includes the time that the solvers were iterating to find a solution. The panel method required the same physical input values but only needed a surface discretization to begin solving. The finite volume solver required a surface mesh as well as a volume mesh that had its own associated time to run. In fact, it was observed that the volume meshing process for the finite volume solver took longer than it took to run the panel method solver (>20 min). In application, this setup time would be included in the time costs associated with design analysis and heavily favors the short setup and run time panel method solvers offer.

At early stages in the aircraft design process, a modified panel method offers a fast solution time with a level of fidelity that matches that of the design. The general aerodynamic trends needed at this stage of the design process will be within the accuracy needed to move forward in the design process.

4. CONCLUSION

4.1 Modified Vortex Panel Method Validation

In this research, 2 inverse Zimmerman planform wings with constant thickness were analyzed using a finite volume solver and 2 different panel method solvers. The results were compared to experimental wind tunnel data gathered using a force balance.

The finite volume solutions showed good agreement with the experimental data. The lift curve demonstrated that this solution technique captured the formation and breakdown of the LEV. As expected, the finite volume solver underestimated the drag coefficient in all cases but captured general trends well. This method offered good predictive capability but took 20-30 times longer than the panel method to iterate and produce results for the same conditions.

The conventional panel method solver was unable to produce any results that matched the finite volume results or experimental data. As expected, because this method did not take into account the LEV produced by LAR wings, it underestimated the lift produced by this wing at increased AoA. Additionally, because a significant amount of the drag produced by these wings is induced due to the high AoAs, it also underestimated the drag produced by these wings. Overall, this further demonstrates the inability of conventional panel method solvers to predict flow characteristics of LAR wings.

The modified panel method solver showed strong agreement with lift characteristics before the LEV breakdown point only after correct calibration of the Kutta condition location. This was done by matching lift curve slopes through moving the Kutta condition further forward when the lift was too low and further aft when the lift was overestimated. Because the lift of these wings is produced at higher angles of attack, the induced drag estimates from this modified panel method matched well at a similar level as the finite volume results. With the inclusion of a skin friction drag estimate within FlightStream, the panel method estimations for total drag show good agreement with wind tunnel force balance data and StarCCM+ finite volume simulations.

Even though there were relatively good predictions of lift and drag coefficient from the modified panel method, there were significant discrepancies found in the moment coefficient. The modified panel method (often, always, most of the time,) correctly predicted a negative relation

between C_M and AoA but failed to capture inflection of the experimental and finite volume results. This discrepancy in C_M results was also visualized in the pressure distributions that showed discrepancies on the lower surface.

The relative accuracy and significantly lower solution times of the panel method lend itself well to early LAR wing design. In design applications this analysis would have reasonable predictions of lift and drag (with the inclusion of a skin friction estimation) while loosely capturing relations seen between moment coefficient and AoA. The fidelity of the analysis would match that of the design at early phase. For predictive capability, the designer would have to use a finite volume analysis or similar wing experimental data to calibrate the Kutta condition definition of the panel method. Overall, a modified panel method shows potential to be used early in the design of LAR aircraft to decrease the development time and cost. Performance would have to be confirmed later in the design process as the level of detail exceeds the accuracy of this method.

4.2 Future Work

There is still more work to be done that allows for the consistent and reliable application of this alternative application strategy of panel method for low aspect ratio wing design. This paper only serves to demonstrate the feasibility of this application strategy. To utilize this tool in practice, further investigation and advancement of this method would be necessary to make it a predictive tool. If achieved, the advantages of low aspect ratio wings could be utilized more fully due to decreased development cost and time.

To achieve make this application strategy more predictive and provide higher confidence in the results there are definite next steps for this research. These include investigating the effects of calibrating the panel method application strategy using a similar wing shape with reference data rather than the exact wing in question. Additionally, investigating the accuracy of using a small set of finite volume solutions would demonstrate accuracy of this alternative calibration source. Finally, having more reference data will always forward the knowledge base of low aspect ratio wing aerodynamic characteristics and allow for predictive relations to be made for Kutta condition location definition.

An investigation into the effects of calibrating this panel method application using a similar wing would show the true effect on result accuracy that the calibration method. If future designers are to use this application strategy, they might be able to get the level of accuracy they need using a similar wing planform and shape with reference data. Knowing how the calibration is affected by calibrating against a similar wing would lead to knowing where the gaps in reference data are for the utilization of this tool for any generic planform.

An investigation into the effect of calibrating this panel method application strategy using a small set of finite volume solutions would also show the level of accuracy of this alternative calibration reference. The lack of experimental reference data would become less significant if the use of finite volume data sets was proven as a reliable calibration reference for this method. This paper currently shows that StarCCM+ is a valid predictive tool for creating small sets of reference data for calibration. In practice, a designer would solve the flow field around their generic LAR wing at 2-3 AoAs and then use those results to calibrate the modified application strategy of panel method to fill in the aerodynamic characteristics for all AoAs up to the stall point.

The testing of physical LAR models will always further the development of this application strategy of panel method. A well-documented wind tunnel experiment with high confidence allows for the use of that data as calibration data in the analysis of LAR wings. With more reference data, there is a higher chance that a designer in the future would be able to use this reference data as a source of calibration.

All previous research opportunities mentioned will allow for relations to be made between geometric features and where the Kutta condition would be applied. With these relations, a designer would be able to apply this modified panel method application strategy in a predictive manner without the need for calibration to another data source. Ultimately, more investigation into the flight characteristics of LAR wings and how they relate to Kutta condition will allow for someone to see relations between the geometric features of the wing and where the Kutta Condition is defined.

BIBLIOGRAPHY

[1] L. M. Nicolai, G. Carichner, and L. M. Nicolai, Fundamentals of aircraft and airship design. Reston, VA: American Institute of Aeronautics and Astronautics, 2010.

[2] D. P. Raymer, Aircraft design: a conceptual approach. Reston, VA: American Institute of Aeronautics and Astronautics, Inc, 2018.

[3] C. H. Zimmerman, “Characteristics of Clark Y Airfoils of Small Aspect Ratios.” NACA-TN431, 1933.

[4] B. Etkin and L. D. Reid, *Dynamics of flight: stability and control*, 3rd ed. New York: Wiley, 1996.

[5] John David Anderson. Fundamentals of aerodynamics. McGraw-Hill Education, 2017.

[6] Stack Exchange, “What is Vortex Lift” https://aviation.stackexchange.com/questions/21069/what-is-vortex-lift

[7] Gunter’s Space Page, Picture of Spaceship 1 https://space.skyrocket.de/doc_lau/spaceshipone.htm

[8] Concorde Technical Specs, Picture of Concorde Planform http://www.concordesst.com/wing.html

[9] Lockhead Martin F-35 Wikipedia, Picture of F-35 https://en.wikipedia.org/wiki/Lockheed_Martin_F-35_Lightning_II

[10] NASA.gov, “Where does the Space Shuttle Land” https://www.nasa.gov/mission_pages/shuttle/behindscenes/shuttle_landing.html

[11] Aerospace Bristol, Activating Concorde’s Nose Droop https://aerospacebristol.org/droop-nose

[12] “EAA Chapter 1 DG2 - Issue #3 Volume#1,” Feb. 6AD.

[13] M. B. Wainfan and M. H. Nieubert, “Mr. Mark D. Moore NASA Langley Research Center Mail Stop 348 Hampton, VA 23681-2199,” Final Report, p. 75, 2004.

[14] P. Jackson, S. Bushell, D. Willis, and J. Winchester, Jane’s all the worlds aircraft: development and production. 2017-2018 / editor, Paul Jackson ; compilers, Susan Bushell, David Willis & Jim Winchester. 2017-2018 / editor, Paul Jackson ; compilers, Susan Bushell, David Willis & Jim Winchester. 2017.

[15] Vought V-173 Wikipedia, Picture of Vought V-173 https://aerospacebristol.org/droop-nose

[16] Pinterest, Dyke Delta Picture, https://www.pinterest.com/pin/132363676519242869/

[17] T. Mueller and G. Torres, “Aerodynamics of Low Aspect Ratio Wings at Low Reynolds Numbers with Applications to Micro Air Vehicle Design,” University of Notre Dame, Notre Dame, Indiana, 2001.

[18] I. H. Abbott and A. E. VonDoenhoff, Theory of wing sections: including a summery of airfoil data, Unabr. and corr. Republ., [Nachdr.]. New York, NY: Dover Publ, 2010.

[19] B. H. Wick, “CHORD WISE AND SPAN WISE LOADING MEASURED AT LOW SPEED ON TRIANGULAR WING HAVING AN ASPECT RATIO OF TWO AND AN NACA 0012 AIRFOIL SECTION.” Ames Aeronautical Laboratory, Moffet Field CA, Jun. 1948.

[20] E. Polhamus, “Concept of the Vortex Lift of Sharp edge.” Langley Research Center, Dec. 1966.

[21] M. V. Ol, “Leading-Edge Vortex Structure of Nonslender Delta Wings at Low Reynolds Number,” p. 11.

[22] S. S. Sathaye, “Lift Distributions on Low Aspect Ratio Wings at Low Reynolds Numbers,” p. 130.

[23] J. Katz and A. Plotkin, *Low-speed aerodynamics: from wing theory to panel methods*. New York: McGraw-Hill, 1991.

[24] S. L. Brunton and C. W. Rowley, “Modeling the unsteady aerodynamic forces on small-scale wings.” Princeton University, Jan. 2009.

[25] H. Werlé, “Hydrodynamic Flow Visualization” Onera, France March 1973

[26] E. N. Tinoco, P. Lu, and F. T. Johnson, “An Improved Panel Method for the Solution of Three-Dimensional Leading-Edge Vortex Flows,” NASA Langley Research Center, vol. 2, no. NAS1-15169, p. 177, 1980.

[27] R. Gordon and J. Rom, “Calculation of Nonlinear Subsonic Characteristics of Wings with Thickness and Camber at High Incidence.” Israel Institute of Technology, Haifa, Isreal, Jun. 1985.

[28] MIT.edu, “5.4 Solutions to Laplace's Equation in Cartesian Coordinates” http://web.mit.edu/6.013_book/www/chapter5/5.4.html

[29] J. M. Luckring, “Reynolds Number, Compressibility, and Leading-Edge Bluntness Efffects on Delta-Wing Aerodynamics.” NASA Langley Research Center, 2004.

[30] Frank M. White. Viscous fluid flow. McGraw-Hill Higher Education, third edition, 2011.